https://doi.org/10.5194/acp-2020-657
Preprint. Discussion started: 7 August 2020

Atmospheric Chemistry and Physics Discussions

Methane mapping, emission quantification and attribution in two European cities; Utrecht, NL and Hamburg, DE

Hossein Maazallahi[1,2], Julianne M. Fernandez[3], Malika Menoud[1], Daniel Zavala-Araiza[1,4], Zachary D. Weller[5], Stefan Schwietzke[6], Joseph C. von Fischer[7], Hugo Denier van der Gon[2], and Thomas Röckmann[1]

[1]Institute for Marine and Atmospheric research Utrecht (IMAU), Utrecht University (UU), Utrecht, The Netherlands
[2]Netherlands Organisation for Applied Scientific Research (TNO), Utrecht, The Netherlands
[3]Department of Earth Sciences, Royal Holloway University of London (RHUL), Egham, United Kingdom
[4]Environmental Defense Fund (EDF), Utrecht, The Netherlands
[5]Department of Statistics, Colorado State University (CSU), United States of America
[6]Environmental Defense Fund (EDF), Berlin, Germany
[7]Department of Biology, Colorado State University (CSU), United States of America

Correspondence to: Hossein Maazallahi (h.maazallahi@uu.nl)

Abstract. Characterizing and attributing methane (CH_4) emissions across varying scales is important from environmental, safety, and economic perspectives, and is essential for designing and evaluating effective mitigation strategies. Mobile real-time measurements of CH_4 in ambient air offer a fast and effective method to identify and quantify local CH_4 emissions in urban areas. We carried out extensive campaigns to measure CH_4 mole fractions at the street level in Utrecht, The Netherlands (2018 and 2019) and Hamburg, Germany (2018). One hundred and forty five leak indications (LIs, i.e., methane enhancements of more than 10% above background levels) were detected in Hamburg and 81 in Utrecht. Measurements of the ethane/methane ratio (C2/C1), methane/carbon dioxide ratio (CH_4/CO_2), and CH_4 isotope composition ($\delta^{13}C$ and δD) show that in Hamburg about 1/3 of the LIs, and in Utrecht 2/3 of the LIs (based on a limited set of C2/C1 measurements), were of fossil fuel origin. We find that in both cities the largest emission rates in the identified LI distribution are from fossil fuel sources. In Hamburg, the lower emission rates in the identified LI distribution are often associated with biogenic characteristics, and partly combustion. Extrapolation of detected LI rates along the roads driven to the gas distribution pipes in the entire road network yields total emissions from sources that can be quantified in the street-level surveys of 440 ± 70 t/yr from all sources in Hamburg, and 150 ± 50 t/yr for Utrecht. In Hamburg, C2/C1, CH_4/CO_2, and isotope-based source attribution analyses shows that 50 - 80 % of all emissions originate from the natural gas distribution network, in Utrecht more limited attribution indicates that 70 - 90 % of the emissions are of fossil origin. Our results confirm previous observations that a few large LIs, creating a heavy tail, are responsible for a significant proportion of fossil CH_4 emissions. In Utrecht, 1/3 of total emissions originated from one LI and in Hamburg >1/4 from 2 LIs. In Hamburg, the local gas utility detected only 20% of the LIs that were identified as from a fossil source, but the largest leaks were located and fixed quickly once the LIs were shared.

1. Introduction

Methane (CH_4) is the second most important anthropogenic greenhouse gas (GHG) after carbon dioxide (CO_2) with a global warming potential of 84 compared to CO_2 over a 20-year time horizon (Myhre et al., 2013). The increase of CH_4 from about 0.7 µmole/mole (parts per million (ppm) or 700 parts per billion (ppb), hereinafter) in pre-industrial times (Etheridge et al., 1998; MacFarling Meure et al., 2006) to almost 1.8 ppm at present (Turner et al., 2019) is responsible for about 0.5 W/m^2 of the total 2.4 W/m^2 radiative forcing since 1750 (Etminan et al., 2016; Myhre et al., 2013). In addition to its direct radiative effect, CH_4 plays an important role in tropospheric chemistry and affects the mixing ratio of other atmospheric compounds, including direct and indirect greenhouse gases, via reaction with the hydroxyl radical (OH), the main loss process of CH_4 (Schmidt and Shindell, 2003). In the stratosphere CH_4 is the main source of water vapor (H_2O) (Noël et al., 2018),

https://doi.org/10.5194/acp-2020-657
Preprint. Discussion started: 7 August 2020

Atmospheric Chemistry and Physics Discussions

which adds another aspect to its radiative forcing. Via these interactions the radiative impact of CH_4 is actually higher than what can be ascribed to its mixing ratio increase alone, and the total radiative forcing ascribed to emissions of CH_4 is estimated to be almost 1 W/m^2, ≈ 60 % of that of CO_2 (Fig 8.17 in Myhre et al., 2013). Given this strong radiative effect, and its relatively short atmospheric lifetime of about 9.1 ± 0.9 yr (Prather et al., 2012), CH_4 is an attractive target for short- and medium-term mitigation of global climate change as mitigation will yield rapid reduction in warming rates.

CH_4 is produced by a wide variety of natural and anthropogenic sources, for example emissions from natural wetlands, agriculture (e.g. ruminants or rice agriculture), waste decomposition, and emissions (intended and non-intended) to the atmosphere that are associated with production, transport, processing, distribution and end-use of oil and natural gas (Heilig, 1994). Fugitive unintended and operation-related emissions occur across the entire oil and natural gas supply chain. In the past decade, numerous large studies have provided better estimates of the emissions from extended oil and gas production basins (Allen et al., 2013; Karion et al., 2013; Omara et al., 2016; Zavala-Araiza et al., 2015; Lyon et al., 2015), the gathering and processing phase (Mitchell et al., 2015), and transmission and storage (Zimmerle et al., 2015; Lyon et al., 2016) in the USA. A recent synthesis concludes that the national emission inventory of the US Environmental Protection Agency (EPA) underestimated supply chain emissions by as much as 60% (Alvarez et al., 2018). McKain et al. (2015) discussed how inventories may underestimate the total CH_4 emission for cities. Also, an analysis of global isotopic composition data suggests that fossil related emissions may be 60% higher than what has been previously estimated (Schwietzke et al., 2016). A strong underestimate of fossil fuel related emissions of CH_4 was also implied by analysis of $\delta^{14}C$-CH_4 in pre-industrial air (Hmiel et al., 2020). These emissions do not only have adverse effects on climate, but also represent an economic loss (Xu and Jiang, 2017) and a potential safety hazard (West et al., 2006).

CH_4 is the main component in natural gas, and the contribution of other compounds varies from one country or region to another. In Europe the national authorities provide specifications on components of natural gas in the distribution network (Table 8 in UNI MISKOLC and ETE, 2008).

Regarding CH_4 emissions from national gas distribution networks (NGDNs), a number of intensive CH_4 surveys with novel mobile and high precision, high precision laser-based gas analyzers in US cities have recently revealed the widespread presence of leak indications (LIs: CH_4 enhancements of more than 10% above background level) with a wide range of magnitudes (Weller et al., 2018; von Fischer et al., 2017; Chamberlain et al., 2016; Hopkins et al., 2016; Jackson et al., 2014; Phillips et al., 2013). The number and severity of natural gas leaks appears to depend on pipeline material and age, local environmental conditions, pipeline maintenance and replacement programs (von Fischer et al., 2017; Gallagher et al., 2015; Hendrick et al., 2016). For example, NGDNs in older cities with a larger fraction of cast iron or bare steel pipes showed more frequent leaks than NGDNs that use the newer plastic pipes. The data on CH_4 leak indications from distribution systems in cities have provided valuable data for emission reduction in the US cities which allows local distribution companies (LDCs) who are in charge of NGDN to quickly fix leaks and allocate resources efficiently (Weller et al., 2018, von Fischer et al., 2017, Lamb et al., 2016; McKain et al., 2015).

Urban CH_4 emissions from European cities are not well known, which requires carrying out extensive campaigns to collect required observations data. Few studies have estimated urban CH_4 fluxes using eddy covariance measurements (Gioli et al., 2012; Helfter et al., 2016) airborne mass balance approaches (O'Shea et al., 2014) and the Radon-222 flux and mixing layer height techniques (Zimnoch et al., 2019). Here we present the result of mobile in-situ measurements at street level for whole-city surveys in two European cities, Utrecht in the Netherlands (NL) and Hamburg in Germany (DE). We quantified emissions in this study using measured CH_4 enhancements above background, which were detected with highly-sensitive CH_4 sensor placed on vehicles. In addition to finding and categorizing the CH_4 enhancements (in a similar manner as done for the US cities in order to facilitate comparability), we made three additional measurements to better facilitate source attribution: the concomitant emission of ethane (C_2H_6) and CO_2, and the carbon and hydrogen isotopic composition of the CH_4. These

https://doi.org/10.5194/acp-2020-657
Preprint. Discussion started: 7 August 2020


Atmospheric Chemistry and Physics Discussions

tracers allow an empirically based source attribution for LIs. In addition to emission quantifications across the urban areas is these two cities, we also quantified CH_4 emissions from some of facilities within the municipal boundary of Utrecht and Hamburg.

2. Materials and methods

2.1. Mobile measurement instrumentation

Mobile atmospheric measurements at street level were conducted using two Cavity Ring-Down Spectroscopy (CRDS) analyzers (Picarro Inc. model G2301 and G4302). The model G2301 instrument provides atmospheric mole fraction measurements of CO_2, CH_4 and H_2O, each of them with an integration time of about 1 sec., which results in a data frequency of ≈ 0.3 Hz for each species. The reproducibility for CH_4 measurements was ≈ 1 ppb for 1 s integration time. The G2301 instrument was powered by a 12 V car battery via a DC/AC converter. The flow rate was ≈187 ml/min. Given the volume and pressure of the measurement cell (volume = 50 ml and pressure ≈ 190 mbar) the cell is flushed approximately every 3 s, so observed enhancements are considerably smoothed out.

The G4302 instrument is a mobile analyzer and provides atmospheric mole fraction measurements of C_2H_6, CH_4 and H_2O at ≈ 1 Hz frequency at a flow rate of ≈ 2.2 L/min using an interior pump with cavity size of 35 ml at controlled pressure of 600 mbar. The additional measurement of C_2H_6 is useful for source attribution since natural gas almost always contains a significant fraction of C_2H_6, whereas microbial sources generally do not emit C_2H_6 (Yacovitch et al., 2014). The G4302 runs on a built-in battery which lasts for about ≈ 6 h. The instrument can be operated in two modes at ≈ 1 Hz frequency for each species: the CH_4-only mode and the CH_4 - C_2H_6 mode. In the CH_4-only mode the instrument has a reproducibility of ≈10 ppb for CH_4. In the CH_4 - C_2H_6 mode the reproducibility is about 100 ppb for CH_4 and 15 ppb for C_2H_6. For Utrecht surveys, the G4302 was not yet available for the initial surveys in 2018, but it was added for the later re-visits (Table S1). For Hamburg, both instruments operated during the entire intensive 3-week measurement campaign in Oct/Nov 2018 (Table S2). The time delay from the inlet to the instruments was measured and accounted for in the data processing procedure. The Coordinated Universal Time (UTC) time shifts between the Global Positioning System (GPS) and the two Picarro instruments were corrected for each instrument in addition to the inlet delay (Table S1 and Table S2).

The instruments were installed on the back seat of a 2012 Volkswagen Transporter (Figure S1). One-quarter inch Teflon tubing was used to pull in air either from the front bumper (0.5 m above ground level) to the G2301 or from the rooftop (2 m above ground level) to the G4302. To avoid dust into the inlets for both instruments, Acrodisc® syringe filter, 0.2 µm was used for G2301 and Parker Balston 9933-05-DQ was used for G4302. The G2301 was used for quantification and attribution purposes and the G4302 mainly for attribution. A comparison of these two instruments is provided in the supplementary information (SI) (Table S3). The vehicle locations were registered using a GPS system that recorded the precise driving track during each survey.

2.2. Target cities: Utrecht and Hamburg

Utrecht is the 4th largest city in the Netherlands with population of approximately 0.35 million inhabitants within an area of roughly 100 km^2. It is located close to the center of the Netherlands and is an important infrastructural hub in the country. The Utrecht city area that we target in this study is well constrained by a ring of highways around the city (A27, A12, A2, and N230) with inhabitants of approximately 0.28 million living within this ring on roughly 45 km^2 of land. Figure S2a shows the streets that were driven in Utrecht and Figure 1a shows the street coverage over four street categories (level 1, 2, 3, residential, and unclassified) obtained from the Open Street Map (OSM; www.openstreetmap.org). The hierarchy of OSM road classes is based on the importance of roads in connecting parts of the national infrastructure. For example, level 1 roads

https://doi.org/10.5194/acp-2020-657
Preprint. Discussion started: 7 August 2020


Atmospheric Chemistry and Physics Discussions

are primarily larger roads connecting cities, residential roads are roads which connect houses and unclassified roads have the lowest importance of interconnecting infrastructure. Moreover, several transects were also made to measure atmospheric mole fraction of CH_4 on the road next to the waste water treatment plant (WWTP) in Utrecht – a potentially larger single source of CH_4 emissions in the city (Table S4).

Hamburg is the 2nd largest city in Germany (about 1.9 million inhabitants, 760 km^2 area) and hosts one of the largest harbors in Europe. The study area in Hamburg is North of the Elbe river (Figure 1b) with ≈1.4 million inhabitants on about 400 km^2 land. Figure S2b shows the streets that were covered in Hamburg and Figure 1b shows the street coverage categorized in the four categories of OSM. Natural gas distribution networks in Hamburg and Utrecht have almost full pipeline coverage beneath the streets. The Hamburg harbor area hosts several large industrial facilities that are related to the midstream / downstream oil and gas sector including refineries and storage tanks. An oil production site (oil well, separator and storage tanks) at Allermöhe (in Hamburg-Bergedorf) was also visited. Information from the State Authority for Mining, Energy and Geology (LBEG, 2018) was used to locate facilities. Precise locations of the facilities surveyed are given in the SI (Table S5). The CH_4 emissions from these locations are estimated but evaluated separately from the emissions found in the rest of the city in order to separate these industrial activities from the NGDNs emissions that were targeted in this study.
The in-situ measurement and GPS data reported here are available on the Integrated Carbon Observation System (ICOS) portal for both cities at the following links: Utrecht and Hamburg (Maazallahi et al., 2020b).

2.3. Driving strategy

The start/end point for each day's measurement surveys across Utrecht and Hamburg were the Institute for Marine and Atmospheric research Utrecht (IMAU; Utrecht University) and the Meteorological Institute (MI; Hamburg University), respectively. From these starting locations, each day's surveys targeted the different districts and neighborhoods of the cities (Table S1 and Table S2). Measurement time periods and survey areas were chosen to select favorable traffic and weather conditions and to avoid large events (e.g., construction; Figure S3), which normally took place between 10 - 18 LT. Average driving speeds on city streets were in the range of 17 ± 7 km/h in Utrecht and 20 ± 6 km/h in Hamburg.

As part of our driving strategy, we revisited locations where we had observed enhanced CH_4 readings. Not all recorded CH_4 mole fraction enhancements are necessarily the result of a stationary CH_4 source. For example, they could be related to mobile sources (e.g., vehicles in the city). Therefore, we revisited a large number of elevated locations in order to confirm the LIs. In contrast to the measurements carried out in many cities in the United States (US) (von Fischer et al., 2017), our measurements were not carried out using Google StreetView cars, but with a vehicle from the IMAU (Figure S1). Due to time and budget restrictions, it was not possible to cover each street at least twice, as done for the US cities. After evaluation of the untargeted first surveys that covered each street at least once, targeted surveys were carried out for verification of observed LIs and for collection of air samples at locations with high CH_4 enhancements. The rationale behind this measurement strategy is that if an enhancement was not recorded during the first survey, it obviously cannot be verified in the second survey. The implications of the difference in the measurement strategy will be discussed in the Results and Discussion sections below.

In total, approximately 1,300 km of roads were driven during Utrecht surveys and about 2,500 km during the Hamburg campaign. In Utrecht, some re-visits were carried out several months to a year after the initial surveys in order to check on the persistence of the LIs. In Hamburg, revisits were also performed within the 4-week intensive measurement period. Further details about the driving logistics are provided in the SI (Table S1 and Table S2). It is possible that pipeline leaks that were detected during the initial survey were repaired before the revisit, and the chance of this occurring increases as the time interval between visits gets longer.

https://doi.org/10.5194/acp-2020-657
Preprint. Discussion started: 7 August 2020

Atmospheric Chemistry and Physics Discussions

2.4. Air sample collections

Samples for isotope analysis of $\delta^{13}C$-CH_4 and $\delta^{2}H$-CH_4 (hereinafter $\delta^{13}C$ and δD respectively) were collected during the revisits at locations that had displayed high CH_4 enhancements during the first surveys. The C_2H_6 information was not used in the selection of sampling locations in order to avoid biased sampling. Samples for isotope analysis were collected in non-transparent aluminum-coated Tedlar 2-liter bags (Supelco, Seupel™ Inert 2L SCV Gas Sampling Bag, and SKC, Standard FlexFoil® Air Sample Bags, 3L) using a 12 V pump and 1/4-inch Teflon tubing. In total, 103 bag samples were collected at 24 locations in Hamburg, 14 of them in the city area North of the Elbe river and 10 at larger facilities. Usually, three individual samples were collected at each source location, plus several background air samples on each sampling day. This sampling scheme generally results in a range of mole fractions that allow source identification using a Keeling plot analysis (Keeling, 1958, 1961). Fossil CH_4 sources in the study areas of this paper (inside the ring for Utrecht and north Elbe in Hamburg) refers to emissions originating from natural gas leaks.

2.5. Meteorological Data

Meteorological information reflecting the large scale wind conditions during the campaigns were obtained from measurements at the Cabauw tower (51.970263 °N, 4.926267 °E) operated by Koninklijk Nederlands Meteorologisch Instituut (KNMI) (Van Ulden and Wieringa, 1996) for Utrecht and Billwerder tower (53.5192 °N, 10.1029 °E) operated by the MI at Hamburg University (Brümmer et al., 2012) for Hamburg. The wind direction and wind speed data from the masts were used for planning the surveys. Pressure and temperature measurements were used to convert volume to mass fluxes for CH_4. We also used information from the towers for the Gaussian plume dispersion model (GPDM) calculations of the emission rates from larger facilities, because the local wind measurements from the 2-D anemometer were not logged continuously.

2.6 Data Evaluation

2.6.1 Data processing

We wrote an automated MATLAB® script (available on GitHub from Maazallahi et al. (2020a)) based on the approach initially introduced in von Fischer et al. (2017), and improved in Weller et al. (2019). It has been demonstrated that the algorithm adequately estimates the majority of emissions from a city (Weller et al., 2018). Using the same algorithm also ensures that results are comparable between European and US cities. The individual steps will be described below. Mapping and spatial analysis were conducted using Google Earth and ESRI ArcMap software.

The first step of the evaluation procedure is quality control of the data from both CH_4 analyzers (e.g. for G4302 in Figure S4a) and the GPS records. Periods of instrument malfunction, instrument flags and unintended signals (e.g. measurement likely from exhaust of other cars, Figure S5) based on notes written during each day's measurements were removed from the raw data. The point to point C_2H_6/CH_4 ratio (C2/C1) calculated from road measurements of a car exhaust shown in Figure S5 is 14.2 ± 7.1 %. During the Utrecht campaign, overall mole percent of CH_4 and C_2H_6 in the NGDN was ≈ 80 % and ≈ 3.9 % and in Hamburg general mole percent of CH_4 and C_2H_6 in the NGDN was about ≈ 95 % and ≈ 3.4 % respectively. This ratio can vary depending on the mixture of gas compositions from different suppliers, but should meet the standards on the gas compositions in the Netherlands (ACM, 2018) and Germany (DVGW, 2013). During the campaigns in Utrecht and Hamburg the C2/C1 of NGDNs was less than 10 % and in our study, we removed all the spots where the C2/C1 ratio was greater than 10 %.

Also, measurements during periods of zero speed (stationary vehicle) and at speeds above 70 km/h were excluded. In order to merge the sharp 1 Hz-frequency records of the GPS with the ≈ 0.3 Hz data from the G2301 analyzer, the CH_4 mole fractions were linearly interpolated to the GPS times. Following the interpolation step, two-time corrections were performed,

https://doi.org/10.5194/acp-2020-657
Preprint. Discussion started: 7 August 2020


Atmospheric Chemistry and Physics Discussions

a correction to the official UTC time and a correction for the delay between air at the inlet and the signal in the CH_4 analyzers. This delay was determined by exposing the inlet to a small CH_4 pulse, ranging from 5-30 seconds depending on the instrument and tubing length. The recorded CH_4 mole fractions were projected back along the driving track according to this delay.

Extraction of the LIs from in-situ measurements requires estimation of the background levels (Figure S8). We estimated CH_4 background as the median value of +/- 2.5 min of measurements around each individual point as suggested in Weller et al. (2019). For estimating the CO_2 background level we used the 5th percentile of +/- 2.5 min of measurements around each individual point (Brantley et al., 2014; Bukowiecki et al., 2002). These background signals were subtracted from the measurement time series to calculate the CH_4 and CO_2 enhancements above background level (Figure S8). For C_2H_6, the background was considered zero as it is normally present at a very low mole fraction; between ~0.4 – 2.5 ppb (Helmig et al., 2016) and this is lower than detection limit of the G4302 instrument.

2.6.2. Quantification of city methane emissions

Weller et al., (2019) established an empirical equation to convert LIs observed with a Picarro G2301 instrument in a moving vehicle in urban environments into emission rates based on large number of controlled release experiments in various environments (Eq. (1)).

$$\text{Ln}(C) = -0.988 + 0.817 * \text{Ln}(Q) \quad (1)$$

In this equation, C represents CH_4 enhancements above the background in ppm and Q is the emission rate in L/min. Weller et al. (2019) used controlled releases to demonstrate that the height of the observed methane enhancement is related to the emission rate and carefully characterized the limitations and associated errors of this equation. We used Eq. (1) to convert CH_4 enhancements encountered during our measurements in Utrecht and Hamburg to emission rates, and we use these estimates to categorize LIs into three classes: high (emission rate > 40 L/min), medium (emission rate 6− 40 L/min) and low (emission rate 0.5 - 6 L/min), following the categories from von Fischer et al. (2017) (Table 1).

The spatial extent of individual LIs was estimated as the distance between the location where the CH_4 mole fraction exceeded the background by more than 10 % (≈ 0.200 ppm; as used in von Fischer et al. (2017) and Weller et al. (2019)) to the location where it fell below this threshold level again. LIs which stay above the threshold for more than 160 m were excluded in the automated evaluation because we suspect that such extended enhancements are most likely not related to leaks from the NGDN (von Fischer et al., 2017).

In a continuous measurement survey on a single day, consecutive CH_4 enhancements above background observed within 5 seconds were aggregated and the location of the emission source was estimated based on the weighted averaging of coordinates (Eq. (2)). Decimal degree coordinates were converted to Cartesian coordinates relative to local references (Figure S9). In Utrecht, the Cathedral tower (Domtoren) and in Hamburg the St. Nicholas' Church were selected as local geographic datums (Table S6). LIs observed on different days at similar locations were clustered and interpreted as one point source when circles of 30 m radius around the center locations overlapped, similar to Weller et al., (2019). The enhancement of the cluster was assigned the maximum observed mole fraction and located as the weighted average of the geographical coordinates of the LIs within that cluster (Eq. (2) from Weller et al. (2019)), where w_i is CH_4 enhancement of each LI.

$$(\text{lon, lat}) = \frac{\sum_{i=1}^{n} w_i * (lon_i, lat_i)}{\sum_{i=1}^{n} w_i} \quad (2)$$

A flow diagram of the evaluation procedure is provided in the SI (Figure S10).

Results from measurement campaigns performed in different cities should be comparable. Therefore, we compared the output of our automated MATLAB® code for two surveys across city centers, one in Utrecht and one in Hamburg, to the evaluation procedure used by Colorado State University (CSU) for the surveys in US cities (von Fischer et al., 2017; Weller et al., 2019). As mentioned above, in our campaign-type studies not all streets were visited twice, so this criterion was dropped

https://doi.org/10.5194/acp-2020-657
Preprint. Discussion started: 7 August 2020

Atmospheric Chemistry and Physics Discussions

from the CSU algorithm. 30 LIs were detected with the two codes and the derived emission rates are very similar (linear fit equation y = 1.00 * x - 0.00, R^2 = 0.99) (Figure S11).

The emission rate per km of road covered during our measurements was then scaled up to the city scale using the ratio of total road length within the study area boundaries derived from OSM to the length of streets covered, and converted to a per-capita emission using the population in the study areas based on LandScan data (Figure S12). Note that in this up-scaling practice, emission quantified from facilities were excluded. We used a Bootstrap method (Nelson, 2008) to estimate emission uncertainties similar to Weller et al. (2018) for the US city studies by resampling from all recorded LIs randomly 30,000 times.

2.6.3. Quantification of methane emissions from larger facilities

Apart from the natural gas distribution network, there are larger facilities in both cities that are potential CH_4 sources within the study area. Several facilities in or around the city areas were visited during the mobile surveys to provide emission estimates (Table S4 and Table S5). These data were evaluated using a simple point source GPDM ( ) (Turner, 1969). We note that emission quantification using GPDM with data from drive-by measurements is prone to large errors (factor of 3 or more) (Yacovitch et al., 2018) especially when the measurements are carried out close to the source. We report the data here since rough emission estimates from facilities other than CH_4 emitting sources can be obtained in the city surveys. Caulton et al. (2018) discuss uncertainties in emission quantification with GPDM. Individual facilities were visited both during the routine each day's screening measurements and during revisits for LI confirmation and air sampling.

In Utrecht, the WWTP is located in the study area and streets around this facility were passed several times during surveys. In Hamburg, we initially performed screening measurements in the harbor area (extensive industrial activities) and near an oil production site and revisited these sites for further quantification and isotopic characterization. The data from the oil production site can be fit reasonably well with a GPDM and were therefore selected for quantification, similar to studies in a shale gas production basin in the USA (Yacovitch et al., 2015) and in the Netherlands (Yacovitch et al., 2018).

$$C(x,y,z) = \frac{Q}{2*\pi*u*\sigma_y*\sigma_z} *\{ \exp\left(\frac{-(z-h)^2}{2*\sigma_z^2}\right) + \exp\left(\frac{-(z+h)^2}{2*\sigma_z^2}\right)\} * \exp\left(\frac{-y^2}{2*\sigma_y^2}\right)\} \quad (3)$$

In Eq. (3), C is the CH_4 enhancement converted to the unit of g/m^3 at cartesian coordinates x, y, and z relative to the source ($[x\ y\ z]_{source} = 0$), x is the distance of the plume from the source aligned with the wind direction, y is the horizontal axis perpendicular to the wind direction, z is the vertical axis, and h is the plume release height. Q is emission rate in g/s, u (m/s) is the wind speed along the x-axis, and σ_y and σ_z are the horizontal and vertical plume dispersion parameters (described below), respectively. Determination of an effective release location is a challenge for the larger facilities. Effective emission locations for each facility were estimated based on wind direction measurements and the locations of maximum CH_4 enhancements. The facilities were generally visited multiple times under different wind conditions. The locations of the maximum CH_4 enhancements were then projected against the ambient wind, and the intersection point of these projections during different wind conditions was defined as effective emission location of the facility. At least two measurement transects with different wind direction were used to estimate the effective location of the source. If wind directions, road accessibility or the shape of plumes were not sufficient to indicate the effective source location, geographical coordinates of centroids of the possible sources using Google Earth imageries and field observations were used to determine the effective emission location.

Cross wind horizontal dispersions σ_y were estimated from the measured plumes by fitting a Gaussian curve to the plumes. A suitable Pasquill–Gifford stability class was then determined by selecting a pair of parameters (Table 1-1 in EPA, 1995) that matches best with the fitted value of σ_y. Vertical dispersions σ_z were then estimated using these Pasquill–Gifford stability classes, using the distances to the source locations (Table 1-2 in EPA, 1995). Uncertainties due to these estimates will be discussed below. Mass emission rates were calculated using the metric volume of CH_4 at 1 bar of atmospheric pressure

https://doi.org/10.5194/acp-2020-657
Preprint. Discussion started: 7 August 2020

Atmospheric Chemistry and Physics Discussions

(0.715 kg/m^3 at 0 °C and 0.666 kg/m^3 at 20 °C, P. 1.124 in IPCC, 1996), and linear interpolation was used for temperatures in between.

2.6.4. Air sampling and source attribution

Depending on the accessibility and traffic, samples were either taken inside the car (Figure S13a) using a tubing from the bumper inlet (Figure S1), or outside the car on foot using the readings from the G4302 to find the best location within the plume (Figure S13b). After collection, the bag samples were returned to the IMAU for analysis of both δ^{13}C-CH_4 and δ^2H-CH_4 (Brass and Röckmann, 2010) and some samples were analyzed at the Royal Holloway University of London (RHUL) for δ^{13}C-CH_4 (Fisher et al., 2006) (Figure S14). The analytical systems for isotope analysis have been described, used and/or compared in several previous publications (Fisher et al., 2011; Röckmann et al., 2016; Umezawa et al., 2018; Zazzeri et al., 2015). Measurement uncertainties in δ^{13}C and δD are 0.05-0.1 ‰ and 2-5 ‰ respectively.

After the LIs were analyzed and quantified, the measurements of C_2H_6, CO_2, and isotopic composition from the air samples were used for source attribution. We characterize the observed LIs as of fossil origin when they had a concomitant C_2H_6 signal between 1 % and 10 % of the CH_4 enhancements and when the isotopic composition was in the range -50 to -40 ‰ for δ^{13}C and -150 to -200 ‰ for δD. CH_4 emissions from combustion processes are always accompanied by large emissions of CO_2 and can therefore be identified based on the low CH_4/CO_2 emission ratio. In this study, LIs with CH_4/CO_2 ratio between 0.02 and 20 with R^2 greater than 0.8 were attributed to combustion. A LI was characterized as microbial when there was no C_2H_6 signal (<1 % of the CH_4 enhancements larger than 500 ppb), δ^{13}C was between -55 ‰ and -70 ‰ and δD was between -260 and -360 ‰ (Figure 7 in Röckmann et al., 2016). LIs with enhancements of CH_4 lower than 500 ppb and no C_2H_6 signals were categorized as unclassified. LIs with no C_2H_6 signals, no significant CH_4/CO_2 ratio, and no information on δ^{13}C and δD were also categorized as unclassified. The source signatures for each sampling location were determined by a Keeling plot analysis of the three samples collected in the plumes and a background sample taken on the same day.

3. Results

3.1. Quantification of CH_4 emissions across Utrecht and Hamburg

Table 2 summarizes the main results from the surveys in Hamburg and Utrecht. The amount of km of roads covered in Hamburg is roughly a factor of 2 larger than in Utrecht, and also the number of detected LIs is roughly a factor of 2 larger, for all three categories. This shows that the overall density of LIs (per km) in both cities is not very different. Specifically, a LI is observed every 5.6 km in Utrecht and every 8.4 km in Hamburg. While not all streets were visited twice in both cities (Table S7 and Table S8) 80 % of LIs in Utrecht and 69 % of LIs in Hamburg were revisited which account for 91 % and 86 % of emissions respectively in the study areas. During revisits, 60 % of CH_4 emissions in Utrecht and 46 % of emissions in Hamburg were verified (e.g. Figure S15). In both cities, all LIs in the high emission category were re-observed. In some cases, re-visits were carried out several months after first detection, and the LIs were still confirmed (Figure S15).

The distribution of CH_4 LIs across the cities of Utrecht and Hamburg is shown in Figure 2. As shown in Table 2, a total of 145 significant LIs were detected in Hamburg and 81 in Utrecht; these LIs cover all three LI categories. Two LIs in Hamburg and one LI in Utrecht fall in the high (red) emission category; the highest LI detected in Utrecht and Hamburg were correspond to emission rates of ≈ 100 L/min and ≈ 70 L/min, respectively. Six LIs in Utrecht and 16 LIs in Hamburg fall in the middle (orange) emission category, and 127 LIs in Hamburg and 74 LIs in Utrecht fall in the low (yellow) emission category. The distribution of emissions over the three categories is also similar between the two cities, with roughly one third of the emissions originating from each category (Figure 2), but the number of LIs in each category is different. The contribution

https://doi.org/10.5194/acp-2020-657
Preprint. Discussion started: 7 August 2020

Atmospheric Chemistry and Physics Discussions

of LIs in the high emission category is about a third of the total observed emissions (35 % in Utrecht is (1 LI) and in 30 % in Hamburg (2 LIs)).

CH_4 emitting locations were categorized based on the roads where the LIs were observed (Figure 1, Figure ***2***Figure 3 and Table S9). Average emission rates per LI as derived from equation (1) are similar for the two cities with 3.6 L/min/LI in Utrecht and 3.4 L/min/LI in Hamburg, but they are distributed differently across the road (Figure 1). In Utrecht, emitting locations on level 2 roads contributed the most (50 % of emissions) to the total emissions while in Hamburg the majority of the emissions occurred on residential roads (56% of total emissions). This shows that the major leak indications may happen on different road classes in different cities and there is no general relation to the size of streets between these two cities.

In Figure 4, we compare cumulative CH_4 emissions for Utrecht and Hamburg to numerous US cities (Weller et al., 2019). After ranking the LIs from largest to smallest, it becomes evident that the largest 5 % of the LIs account for about 60 % of emissions in Utrecht, and 50 % of the emissions in Hamburg.

As mentioned above, the observed total emission rates observed on roads in urban environment in the two cities are relatively similar when normalized by the total amount of km covered, 0.64 L/min/km for Utrecht and 0.4 L/min/km for Hamburg (Table 2). Using these two emission factors, the observed emission rates (110 t/yr in Utrecht and 180 t/yr in Hamburg) were up-scaled to the entire road network in the two cities, ≈ 650 km in Utrecht and ≈ 3,000 km in Hamburg. This includes the implicit assumption that the pipeline network is similar to the street network. Total up-scaled emission rates based on mobile measurements on roads in urban environment before considering attribution analysis over LI locations are 150 t/yr and 440 t/yr across the study areas of Utrecht and Hamburg respectively. Distributing the calculated emission rates over the population in the city areas yields emission rates of 0.54 ± 0.15 kg/yr/capita for Utrecht and 0.31 ± 0.04 kg/yr/capita for Hamburg.

3.2. Attribution of CH_4 emissions across Utrecht and Hamburg

Figure 5 shows the results of the isotope analysis for the 21 locations in Hamburg where acceptable Keeling plots were obtained (Table S10 and Table S11). The results cluster mostly in three groups, which are characterized by the expected isotope signatures for fossil, microbial, and pyrogenic samples as described in Röckmann et al., (2016).

Average isotope signatures for the LIs in the city of Hamburg were $\delta^{13}C$ = -52.3 ± 5.1 ‰ and δD = -298.4 ± 30.3 ‰ for the samples characterized as microbial and $\delta^{13}C$ = -41.9 ± 1.0 ‰ and δD = -196.1 ± 10.6 ‰ for the samples characterized as fossil (Figure 5). One sample from the Hamburg city area displays a very high $\delta^{13}C$ and δD source signatures around -23 ‰ and -153 ‰ respectively. The origin of CH_4 with such an unusual isotopic signature could not be identified and it is considered an outlier. In Hamburg, 10 % of the LI locations (38 % of emissions) on the north side of Elbe were sampled for isotope analysis. The lab isotopic attributions show that the LIs with the higher emission rates are mostly caused by emission of fossil CH_4. 79 % of the inferred emissions at 38 % of the LIs were identified as of fossil origin, 20 % of emissions at 54 % of the LIs as of microbial origin (for an identified source see Figure S16), 1 % of emissions at 8% of LIs as of pyrogenic origin. In Hamburg, during three passes through the new Elbe tunnel (Figure S6) a CH_4/CO_2 of 0.2 ± 0.1 ppb/ppm was derived for combustion, related emission. During the surveys of open roads, clear CH_4/CO_2 correlations were observed for several LIs and an example of a measurement of car exhaust is shown in Figure S7a with CH_4/CO_2 = 1.6 ppb/ppm. Previous studies have shown relatively low CH_4/CO_2 ratios of $4.6*10^{-2}$ ppb/ppm (Popa et al., 2014), 0.41 ppb/ppm (E. K. Nam et al., 2004), and 0.3 ppb/ppm (Naus et al., 2018) when cars work under normal conditions. During cold engine (Naus et al., 2018) or incomplete combustion conditions, the fuel to air ratio is too high, which results in enhanced emission of black carbon particles and reduced carbon compounds, so higher CH_4/CO_2 ratios. Hu et al. (2018) reported 2 ± 2.1 ppb/ppm in a tunnel, but 12 ± 5.3 ppb/ppm on roads. In addition to car exhaust, there are other combustion sources which can affect CH_4 and CO_2 mole fractions at the street level including natural gas water heater (CH_4/CO_2 ratio of ≈ 2 ppb/ppm; Lebel et al., 2020), restaurant kitchens,

https://doi.org/10.5194/acp-2020-657
Preprint. Discussion started: 7 August 2020

Atmospheric Chemistry and Physics Discussions

etc. Based on the criteria defined above, 17% of LIs (10% of emissions) can be attributed to combustion with a mean CH_4/CO_2 ratio of 3.2 ± 3.9 ppb/ppm (max = 18.7 and min = 0.8 ppb/ppm). The C2/C1 ratio for these LIs attributed to combustion in Hamburg was 7.8 ± 3.5 %. In Utrecht 7 % of LIs (2 % of emissions) are attributed to combustion with a mean CH_4/CO_2 ratio of 9.8 ± 5.8 ppb/ppm (max = 16.7 and min = 3.0 ppb/ppm).

Based on the C_2H_6 signals, 64 % of the emissions (33 % of LIs) were characterized as fossil, while 25 % of emissions (20 % of LIs) were identified as microbial. Due to low CH_4 and C_2H_6 enhancements, 47 % of the locations (11 % of emission) were considered unclassified. The C2/C1 ratio for the LIs attributed to emissions from NGDNs in Hamburg study area (North Elbe) is 4.1 ± 2.0 %. The oil production site in south-east Hamburg had a higher C2/C1 ratio of 7.1 ± 1.5 %.

In Utrecht, C_2H_6 was measured only during four surveys in February, April, and June 2019 (revisits of 2-day surveys across the city center and 2 days to LIs with high emission rates) as the CH_4/C_2H_6 analyzer was not available during the first campaign. The C2/C1ratios from this limited survey indicates that 93 % of emissions (69 % of the LIs across the city centre, including combustions) are likely from fossil sources (Table 2) and 73 % of emissions (43% of the LIs, including combustion) out of all LIs. In Utrecht, the C2/C1 ratio for the LIs attributed to NGDNs is 3.9 ± 0.8 %.

3.3. Quantification and Attribution of CH_4 plume from larger facilities

Table 3 shows the estimates of emission rate from the larger facilities in Utrecht and Hamburg. CH_4 plumes from the WWTP (Figure 6 and Table S4) were intercepted numerous times during the city transects, and the error estimate in Table 3 represents one standard deviation of 5 sets of measurements where each measurement comprises 2-4 transects during three measurement days (12-Feb.-2018, 24-Apr.2018, and 07-Jan.-2019). Figure 7 shows an example of a fit of a Gaussian plume to the measurements from the Utrecht WWTP. The derived distance to the source was 215 m, the hourly average wind speed was 3.5 m/s and the wind direction was 178 ± 5 degrees (Table S4). The total emission rate of the WWTP in Utrecht was estimated at 160 ± 80 t/yr. The reported errors include stability classes, wind speed and directions, and effective point source coordinates. Not all transects provided datasets that allowed an adequate Gaussian fit, these were not included in total estimates from the facilities, e.g. measurements during the visits of the harbor area in Hamburg were excluded. In Hamburg, plumes from several facilities were also intercepted several times (Table S5), and for a Compost and Soil Company in Hamburg we estimate an emission rate of 60 ± 40 t/yr. The drive-by quantifications at the upstream sites in Hamburg from a separator, a tank, and an oil well yield annual CH_4 emission of 4.4 ± 3.6 t/yr, 3.7 ± 1.9 t/yr, and 4.8 ± 3.9 t/yr respectively.

4. Discussion

As mentioned above, we used methods similar to the ones introduced by von Fischer et al. (2017) and updated in Weller et al. (2019) that were used to characterize CH_4 emission from local gas distribution systems in the US. An important difference is that we did not visit each street twice in the untargeted survey, and the revisits were specifically targeted at locations where we had found a LI during the first visit. A consequence of the different sampling strategy is that we do not base our city-level extrapolated emissions estimates on "confirmed" LIs, as done in Weller et al. (2019) but on all the LIs observed. In our study, 60 % of CH_4 LIs in Utrecht and 46 % of LIs in Hamburg were confirmed. This number may be biased high, since we preferentially revisited locations that had shown higher LIs, and the percentage of confirmed LIs may have been lower if we had visited locations with smaller LIs. von Fischer et al. (2017) reported that LIs in the high emission rate category have a 74 % chance of detection, which decreased to 63 % for the middle category and 35 % frequency for the small category. In our study, all LIs within the high emission rate category (n = 1 and n = 2 LIs in Utrecht and Hamburg respectively) were confirmed in both cities. Overall, the confirmation rates found in Hamburg and Utrecht were similar to the ones reported

https://doi.org/10.5194/acp-2020-657
Preprint. Discussion started: 7 August 2020


Atmospheric Chemistry and Physics Discussions

in the US cities by von Fischer et al. (2017), suggesting that the results from both driving strategies can be compared, assuming an overall confirmation percentage of roughly 50%.

In 13 US cities the "LI density" ranged from 1 LI per 1.6 km driven to 1 LI per ≈ 320 km driven (EDF, 2019). This illustrates that cities within one country can be very different in their NGDN infrastructure. In Utrecht, one LI was observed every 5.6 km of street covered and in Hamburg every 8.4 km covered. Note that we normalize the number of LIs per km of road covered, not km of road driven, since the revisits were targeted to confirm LIs, which would bias the statistics if we normalize by km of road driven. After accounting for the confirmation percentage of about 50%, the LI densities in Utrecht and Hamburg become 1 LI per 11.2 km covered in Utrecht, and 1 LI per 16.8 km covered in Hamburg. When we take into account the attributions (fraction fossil/total LIs is 43 % in Utrecht and 31 % in Hamburg), confirmed LIs from the NGDN are found every 26 km in Utrecht and every 54 km in Hamburg. The highest 1% of the LIs in Utrecht and Hamburg account for approximately 30 % of emissions, emphasizing the presence of a skewed distribution of emissions. The emissions distribution is even more skewed for these two European cities than for countrywide US cities, where approximately 25 % of emissions comes from the highest 5 % of the LIs. Skewed emission distributions appear to be typical for emissions from the oil and gas supply chain across different scales. For example, a synthesis study reviewing the distribution of upstream emissions from the US natural gas system shows that in the US 5% of the leaks are responsible for 50 % of the emissions (Brandt et al., 2016).

Four different approaches were combined in Hamburg for source attribution, which allows an evaluation of their consistency. Figure 5 shows that measurements of the C2/C1, δD, and $\delta^{13}C$ provide a very consistent distinction between fossil and microbial sources of CH_4. Except for one outlier with a very high $\delta^{13}C$ and δD contents but no C_2H_6 signal, all samples that are classified as "microbial" by a low $\delta^{13}C$ and δD signatures contain no measurable C_2H_6, and all samples that would be characterized as "fossil" based on $\delta^{13}C$ and δD do show a concomitant C_2H_6 signal. This strengthens the confidence in source attribution using these tracers. The fossil $\delta^{13}C$ signature of bag samples from natural gas leaks in Hamburg ($\delta^{13}C$ = -41.9 ± 1.0 ‰) is higher than recently reported in the city of Heidelberg ($\delta^{13}C$ = −46.1 ± 0.8 ‰ (Hoheisel et al., 2019)). This shows that within one country $\delta^{13}C$ from NGDN can vary from one region to another. This could be the result of differences in the mixture of natural gas from various suppliers for different regions in Germany (DVGW, 2013), or for different times of the year, or both.

In Hamburg both C2/C1 and CH_4/CO_2 analysis along with $\delta^{13}C$ and δD signatures suggest that ≈ 50 % to ≈ 80 % of estimated emissions (≈ 30 % and ≈ 40 % of LIs respectively) originate from NGDNs, whereas CH_4/CO_2 analysis and the smaller sample of C2/C1 measurements in Utrecht suggests that the overwhelming fraction (70 - 90 % of emissions; 40 – 70 % % of LIs) originated from NGDNs. We note that although it is widely assumed that microbial CH_4 is not associated with ethane, some studies that have reported microbial production of ethane, so it may not be a unique identifier (Davis and Squires, 1954; Fukuda et al., 1984; Gollakota and Jayalakshmi, 1983; Formolo, 2010). The online C2/C1 analysis to attribute LIs is fast and can be used at larger scale, but with the instrument we used we were not able to clearly attribute sources with CH_4 enhancements of less than 500 ppb. Isotopic analysis by IRMS can attribute sources for smaller LIs (down to 100-200 ppb) but is clearly more labor intensive, and it would be a considerable effort to take samples from all LIs observed across an urban area.

In Hamburg, most LIs were detected in the city center (Figure 2). This means that the LI density is higher than the average value in the center, but much lower than the average value in the surrounding districts and residential areas. Many of the LIs in the city center were attributed to combustion and microbial sources, thus they do not originate from leaks in the NGDN. Many of the microbial LIs encountered in Hamburg are around the Binnenalster lake (Figure S16), which suggests that anaerobic methanogenesis (Stephenson and Stickland, 1933; Thauer, 1998) is an important source of CH_4 emissions in this area.

https://doi.org/10.5194/acp-2020-657
Preprint. Discussion started: 7 August 2020


Atmospheric Chemistry and Physics Discussions

In the national inventory reports, total upscaled emissions from NGDNs are based on sets of emission factors for different pipeline materials (e.g. grey cast iron, steel, or plastic) at different pressures (e.g. <= 200 mbar or >200 mbar). The reported emission factors are based on IPCC tier 3 approach (Buendia et al., 2019). However, emission estimates do not exist for individual cities including Utrecht and Hamburg. Also, it is not possible to calculate a robust city-level estimate using the nationally reported emission factors because there is no publicly available activity data for associated activity data, i.e., pipeline materials and lengths for each material, at the level of individual cities. As a result, a robust direct comparison between nationally reported emissions and our measurements, akin to a recent study in the United States (Weller et al., 2020), is currently not possible. The following juxtaposition of our estimates and national inventory downscaling to city-level is therefore provided primarily as illustration of the data gaps rather than a scientific comparison. In Utrecht, we attributed 70 – 90 % of the mobile measurement inferred emissions of ≈ 150 t/yr to the NGDN, thus 105 – 135 t/yr. The national inventory report from National Institute for Public Health and the Environment (RIVM) in the Netherlands used measurements of 65 leaks from different pipeline materials and pressures in 2013, to derive an average emission factor (weighted by pipeline material and pressure) for emission from the NGDN of ≈ 110 kg/km/yr (max = 230 kg/km/yr (grey cast iron) and min = 40 kg/km/yr (other material with pressure of <= 200 mbar)) (P. 130 in Peek et al. (2019)), which results in average CH_4 emissions of ≈ 70 t/yr (min = 30 t/yr and max = 150 t/yr) for the study area of Utrecht, assuming ≈ 650 km of pipelines inside the ring of Utrecht, and further assuming that Utrecht's NGDN is representative of the national reported average (see qualifiers above). The average emissions for the Utrecht study based on emissions factors reported for the Netherlands is smaller by a factor of 1.5 - 2 than the emissions derived here, but the factor of 5 variability in the reported emissions (resulting from the variability in pipeline materials) highlights the need for city-level specific activity data for a robust comparison. In Hamburg 50 – 80 % of the upscaled emissions of 440 t/yr (220 – 350 t/yr), can be attributed to the emission from NGDN. The national inventory from the Federal Environment Agency (UBA) in Germany, reports an average CH_4 emission factor for NGDN from low pressure pipelines as ≈ 290 kg/km/yr (max = 445 kg/km/yr (grey cast iron) and min = 51 kg/km/yr (plastic)) based on measurements from the 1990s (Table 169 in Federal Environment Agency (2019)). Assuming ≈ 3000 km pipelines in our target region, and further assuming that Hamburg's NGDN is representative of the national reported average (see qualifiers above), results in average estimated CH_4 emissions from NGDN of ≈ 870 t/yr (min = 155 t/yr and max = 1350 t/yr). While this study's estimate of 220 – 350 t/yr falls in the lower end of this range, the factor of 9 variability in the reported emissions (resulting from the variability in pipeline materials) highlights again the need for city-level specific activity data for a robust comparison. To put the national inventory comparison in perspective, it should be noted that the LDC in Hamburg (GasNetz Hamburg (https://www.gasnetz-hamburg.de)) detected and fixed leaks at 20 % of the fossil LIs in this study, which accounted for 50 % of emissions. In Utrecht and Hamburg, the natural gas consumption in our target area were retrieved through communications with LDCs. In Utrecht and Hamburg study areas, the natural gas consumption is 0.16 bcm/yr (STEDIN (https://www.stedin.net/), personal communication) and 0.75 bcm/yr (GasNetz Hamburg, personal communication) respectively. The emissions from NGDNs estimated in our study in Utrecht is between 0.10 – 0.12 % and in Hamburg is between 0.04 – 0.07 % of total annual natural gas consumptions in the same area. Weller et al. (2020) reported 0.69 Tg/year (0.25 - 1.23 with 95 % credibility interval) emissions from local distribution network in the US where majority of natural gas consumptions are from residential and commercial sectors with sum of ≈ 170 Tg/year (U.S. EIA, 2019) which shows 0.4 % (0.15 % - 0.7 %) loss from NGDNs in the US. The loss from NGDNs in the US is about four times higher than the loss in Utrecht and about ten times higher than the loss in Hamburg reported in this study. Natural gas consumption densities in Utrecht and Hamburg study area are ≈ 570 m^3/capita/yr and ≈ 520 m^3/capita/yr and in the US is about ≈ 730 m^3/capita/yr considering populations of ≈ 0.28 million and ≈ 1.45 million in Utrecht and Hamburg (Figure S12) and ≈ 330 million in the US (US Census Bureau, 2020). This shows that annual natural gas consumptions per capita in the US is about 30 % and 40 % higher than Utrecht and Hamburg respectively. The emission per km pipeline in Utrecht is between

https://doi.org/10.5194/acp-2020-657
Preprint. Discussion started: 7 August 2020


Atmospheric Chemistry and Physics Discussions

481 0.45 – 0.5 L/min/km and in Hamburg is between 0.2 – 0.32 L/min/km. In the US based on 2,086,000 km pipeline for local
482 natural gas distribution network (Weller et al., 2020) this emission factor will be between 0.32 – 1.57 L/min/km. This shows
483 higher emissions per km pipeline in the countrywide studies of US compared to just two European cities of Utrecht and
484 Hamburg (see qualifiers above). This can be partly explained by pipeline material, maintenance protocols, and higher use of
485 natural gas consumption in the US. However, the substantial variability in emission rates across US cities – as wells as the
486 variability of gas consumption over the year – again restricts a comparison of two cities with a national average measured over
487 multiple years.
488 Normalized LIs emissions per capita in Utrecht (0.54 ± 0.15 kg/yr/capita) are almost double the emission factor in
489 Hamburg (0.31 ± 0.04 kg/yr/capita). This metric may be useful to compare cities, assuming that the emission quantification
490 method is equally effective in different cities. CH_4 emissions in different cities can be different due to several factors. For
491 example, main factors can be gas pipeline age and material, sewer system. In our study we only surveyed two cities, and the
492 above number may not be adequate for extrapolation to the country scale (McKain et al., 2015).
493 After the city surveys, locations with the highest emissions (high and medium categories) were shared with the
494 STEDIN Utrecht and all LI locations were reported to the GasNetz Hamburg. The utilities repair teams were sent to check
495 whether LIs could be detected as leaks from NGDN and fixed. The LDCs follow leak detection procedures based on country
496 regulations (e.g., for GasNetz Hamburg in Table S12). GasNetz Hamburg also co-located the coordinates of the detected
497 reported LIs with the NGDN and prioritized repairs based on safety regulations mentioned in Table S13. This interaction with
498 the LDCs resulted in fixing major NGDN leaks in both cities. In Utrecht the only spot in the high emission category was
499 reported to STEDIN, but the pipelines on this street had been replaced and the gas leak was most likely fixed as a result of the
500 replacement by STEDIN, as it was not found later by the gas company nor in our later survey with the CH_4 / C_2H_6 analyzer.
501 In Utrecht, half of the LIs in the medium category were found and repaired.
502 A routine leak survey (detection and repair) had been performed by GasNetz Hamburg between 1-5 months before
503 the campaign, for the different regions. The timing of any routine detection and repair likely influences the absolute number
504 of LIs measured during independent mobile measurements, and the survey by GasNetz Hamburg thus likely has influenced
505 the absolute number of LIs measured in our campaign. We then reported the LI latitude/longitude coordinates to GasNetz
506 Hamburg about 4 months after our campaign (additionally, we provided map images of the LIs immediately after the
507 campaign). The comparison of the number of reported LIs (and emission rates) during our campaign with those identified by
508 GasNetz Hamburg post-campaign assumes that the leaks continued to emit until they were detected and fixed by GasNetz
509 Hamburg (if they were detected).
510 Depending on how close the gas leaks are to buildings, LDCs prioritize the leaks into four classes from the highest
511 to lowest priority: A1, A2, B, and C (Table S13). In Hamburg, both LIs in the high category were identified as A1 gas leaks
512 and fixed by GasNetz Hamburg immediately. Most of the LIs that were detected and identified as fossil in Hamburg are in
513 close proximity to the natural gas distribution pipelines (Table S14). Investigation of the pipeline material shows that most of
514 NGDN emissions are due to leaks from steel pipelines (Table S15), which are more prone to leakage because of pipeline
515 corrosion (Zhao et al., 2018). Nevertheless, only 7 of the 30 LIs (23%) that were positively attributed to fossil CH_4 were
516 detected and fixed by the LDC. If we assume that the fraction fossil / total LIs determined in Hamburg (≈ 35%) is representative
517 for the entire population of LIs encountered (thus also for the ones that were not attributable), about 50 of the 145 LIs are
518 likely due to fossil CH_4. The LDC found and fixed leaks at 10 of these locations (≈ 20%). A recent revisit (January 2020) to
519 these locations confirmed that no LIs were detected at 9 out of these 10 locations. For the 10th location a smaller LI was
520 detected in close proximity, and GasNetz Hamburg confirmed that this was a leak from a steel pipeline. The whole pipeline
521 system on this street dates back to the 1930s and is targeted for replacement in the near future.

https://doi.org/10.5194/acp-2020-657
Preprint. Discussion started: 7 August 2020


Atmospheric Chemistry and Physics Discussions

In summary, about 20 % of the LIs including the two largest LIs that were attributed to a fossil source were identified as gas leaks (Figure S17) and repaired by GasNetz Hamburg but these accounted for about 50 % of fossil CH_4 emissions of Hamburg, similar to what was observed in the US studies (Weller et al., 2018). Possibly, smaller leakages that can be detected with the high sensitivity instruments used in the mobile surveys cannot be detected with the less sensitive equipment of LDCs. Another possible explanation for the fact that the LDC did not detect more leaks may be that reported LI locations do not always coincide with the actual leak locations, although Weller et al. (2018) reported that the median distance of actual leak locations to the reported ones was 19 m. Combined measurements with GasNetz Hamburg are planned to investigate why the majority of the smaller LIs reported in mobile surveys is not detected in the regular surveys of the LDC.

The average C2/C1 ratio for LIs with a significant C_2H_6 signals across Hamburg was 5.6 ± 3.9 %. For the spots where the LDC found and fixed leaks this ratio was 3.9 ± 2.6 %. Thus, some of the locations were CH_4 enhancements were found were influenced by sources with an even higher C2/C1 ratio than the gas in the NGDN. One confirmed example is the very high ratio found in exhaust from a vehicle as shown in as shown in Figure S5. The abnormal operation of this vehicle is confirmed by the very high CH_4/CO_2 ratio of 5.5 ppb/ppm (SI, section S2). This is more than 20 times higher than CH_4/CO_2 ratios of 0.2 ± 0.1 ppb/ppm observed during passages through the Elbe tunnel, a ratio that agrees with previous studies (SI, section S2).

Repairing gas leaks in a city has several benefits for safety (preventing explosions), sustainability (minimizing GHG emissions) and economics. Gas that is not lost via leaks can be sold for profit, but gas leak detection and repair is expensive and is usually associated with interruptions of the infrastructure (breaking up pavements and roads). Also, as reported above, and in agreement with the studies in US cities, for small LIs the underlying leaks are often not found by the LDCs, possibly because their equipment is less sensitive and aimed for finding leak rates that are potentially dangerous.

Our measurements in Hamburg demonstrate that in particular smaller LIs may originate from biogenic sources, e.g. the sewage system, and not necessarily from leaks in the NGDN. In this respect, attribution of LIs prior to reporting to the LDCs may be beneficial to facilitate effective repair and in Figure S18 we suggest an optimized protocol for emissions reduction from the NGDN in cities.

The WWTP in Utrecht emits 160 ± 80 t/yr, which is similar to the total detected emissions (150 t/yr) inside the study area of Utrecht. The emissions reported for this facility from 2010 until 2017 are 130 ± 50 t/yr (Rijksoverheid, 2019), in good agreement with our measurements. CH_4 emission from a single well in Hamburg was estimated at 0.5 ± 0.4 kg/hr, which is in the range of median emissions of 0.26 kg/hr reported for gas production wells in Groningen, NL (Yacovitch et al., 2018), and average emissions of all US oil and gas production wells 0.9 ± 0.2 kg/hr (Alvarez et al., 2018). In Hamburg, the emissions from a Compost and Soil Company amount to about 10 % of the total emissions in the city target region, whereas a wellhead, a storage tank and a waste-oil separator contribute only about 1 % each. This shows that individual facilities can contribute significantly to total emissions in a city. The contribution of each source is dependent on infrastructure, urban planning and other conditions in the city (e.g. age and material of pipeline, maintenance programs, waste management, sewer system conditions, etc.), which may change the source mix from one city to another. For example, in Utrecht the WWTP is located within our domain of study. The wastewater treatment in Hamburg most likely causes CH_4 emissions elsewhere. Therefore, facility-scale CH_4 emissions should be reported on a more aggregated provincial or national level. For emissions from the NGDN the urban scale is highly relevant, as the emission can only be mitigated at this scale.

5. Conclusions

Mobile measurements provide a fast and accurate technique for observing and identifying even relatively small CH_4 enhancements (i.e., tens of ppb) across cities and are useful for detecting potential gas leaks. During our intensive measurement campaigns, 81 LIs were observed in Utrecht (corresponding to emissions of about 107 t CH_4 / yr) and 145 LIs (≈180 t CH_4 /

https://doi.org/10.5194/acp-2020-657
Preprint. Discussion started: 7 August 2020

Atmospheric Chemistry and Physics Discussions

yr) in Hamburg. These emissions estimates were up-scaled to total emissions of 150 t/yr in Utrecht and 440 t/yr in Hamburg. The isotopic signature of CH_4 in air samples and continuous mobile measurement of CO_2 and C_2H_6 mole fraction show that not all the LIs observed across the two cities have fossil origin. In Utrecht, C2/C1 and CH_4/CO_2 analyses show that 70 -90 % of emissions were fossil. In Hamburg, C2/C1, CH_4/CO_2, and $\delta^{13}C$-δD analyses suggests that 50 - 80 % of emissions originate from natural gas pipelines. For the locations where samples for isotope analysis were collected, 80 % of emissions were identified as fossil. A large fraction of emissions in both cities were from few high emitting locations. The LDC in Hamburg (GasNetz Hamburg) detected and fixed leaks at 20 % of the locations that likely due to fossil sources, but these accounted for 50 % of emissions. Large LIs were generally confirmed as gas leaks from steel pipelines. The C2/C1 ratio at the locations where gas leaks were fixed by GasNetz Hamburg was 3.9 ± 2.6 %. The mobile measurement technique is less labor and time intensive than conventional methods and can provide extensive coverage across a city in a short period. Based on our experience for the Netherlands and Germany a protocol could be developed that aids LDCs in guiding their leak detection and repair teams. The use of emission categories and source attribution can help target repair activities to the locations of large fossil emissions. Emission quantification from large facilities shows that these emissions may be equivalent to total CH_4 emissions from NGDN leaks in urban environments. In order to analyze discrepancies between spatial explicit measurement-based estimates as presented here with reported annual average national emissions by sectors a coordinated effort with national agencies is necessary to address the lack of publicly available activity data (e.g., pipe material) disaggregated from the national-level (e.g., at the city-level).

Author contributions

H. M. performed the mobile measurements, wrote the MATLAB® code, analyzed the data, and together with T. R. drafted the manuscript. J. M. F. and M. M. contributed with air sampling and isotope analysis. D. Z. A. and S. S. contributed to the scientific interpretation and comparison between European and US cities. Z. D. W. and J. C. v. F. facilitated comparison to US cities and contributed to the statistical analysis. H. D. v. d. G. and T. R. provided instruments, equipment, and supervised the measurements and data analysis. T. R. developed the research idea and coordinated the city campaigns. All authors contributed to the interpretation of the results and the improvement of the manuscript.

Competing interests: The authors declare that they have no conflict of interest.

Acknowledgements

This work was supported by the Climate and Clean Air Coalition (CCAC) Oil and Gas Methane Science Studies (MMS) hosted by the United Nations Environment Programme. Funding was provided by the Environmental Defense Fund, Oil and Gas Climate Initiative, European Commission, and CCAC. This project received further support from the H2020 Marie Skłodowska-Curie project Methane goes Mobile – Measurements and Modelling (MEMO^2; https://h2020-memo2.eu/), grant number 722479. We thank Dr. Rebecca Fisher who supervised RHUL contribution to the isotopic analysis of Hamburg campaign. Special thanks to Prof. Stefan Bühler from the Meteorological Institute of Hamburg University and Dr. Stefan Kinne from the Max Planck Institute for Meteorology for hosting our team during the Hamburg city measurement surveys. We appreciate continuous efforts from executive and management boards of GasNetz Hamburg, Dr. Luise Westphal, Michael Dammann, Dr. Ralf Luy, and Christian Feickert who facilitated productive communications, provided information on the gas infrastructure in Hamburg and organized leaks repairs with their teams in study area of Hamburg. We also thank asset manager of STEDIN Utrecht, Ricardo Verhoeve who provided information and planned leaks repairs by STEDIN in Utrecht. We thank Charlotte Große from DBI Gas and Environmental Technologies GmbH Leipzig (DBI GUT Leipzig) who helped with clarifying information on reported emission factors provided in national inventory reports. We thank the former MSc students of Utrecht University, Laurens Stoop and Tim van der Akker who helped with the measurements in Utrecht study area.

https://doi.org/10.5194/acp-2020-657
Preprint. Discussion started: 7 August 2020

Atmospheric Chemistry and Physics Discussions

References

ACM: Authority for Consumers and Markets in the Netherlands, Low NOx Burgners (LNBs) gas code, [online] Available from: https://wetten.overheid.nl/BWBR0037935/2018-05-26, 2018.

Allen, D. T., Torres, V. M., Thomas, J., Sullivan, D. W., Harrison, M., Hendler, A., Herndon, S. C., Kolb, C. E., Fraser, M. P., Hill, A. D., Lamb, B. K., Miskimins, J., Sawyer, R. F. and Seinfeld, J. H.: Measurements of methane emissions at natural gas production sites in the United States, Proc. Natl. Acad. Sci., 110(44), 17768–17773, doi:10.1073/pnas.1304880110, 2013.

Alvarez, R. A., Zavala-Araiza, D., Lyon, D. R., Allen, D. T., Barkley, Z. R., Brandt, A. R., Davis, K. J., Herndon, S. C., Jacob, D. J., Karion, A., Kort, E. A., Lamb, B. K., Lauvaux, T., Maasakkers, J. D., Marchese, A. J., Omara, M., Pacala, S. W., Peischl, J., Robinson, A. L., Shepson, P. B., Sweeney, C., Townsend-Small, A., Wofsy, S. C. and Hamburg, S. P.: Assessment of methane emissions from the U.S. oil and gas supply chain., Science, 361(6398), 186–188, doi:10.1126/science.aar7204, 2018.

Brandt, A. R., Heath, G. A. and Cooley, D.: Methane Leaks from Natural Gas Systems Follow Extreme Distributions, Environ. Sci. Technol., 50(22), 12512–12520, doi:10.1021/acs.est.6b04303, 2016.

Brantley, H. L., Hagler, G. S. W., Kimbrough, E. S., Williams, R. W., Mukerjee, S. and Neas, L. M.: Mobile air monitoring data-processing strategies and effects on spatial air pollution trends, Atmos. Meas. Tech., 7(7), 2169–2183, doi:10.5194/amt-7-2169-2014, 2014.

Brass, M. and Röckmann, T.: Continuous-flow isotope ratio mass spectrometry method for carbon and hydrogen isotope measurements on atmospheric methane, Atmos. Meas. Tech., 3(6), 1707–1721, doi:10.5194/amt-3-1707-2010, 2010.

Brümmer, B., Lange, I. and Konow, H.: Atmospheric boundary layer measurements at the 280 m high Hamburg weather mast 1995-2011: mean annual and diurnal cycles, Meteorol. Zeitschrift, 21(4), 319–335, doi:10.1127/0941-2948/2012/0338, 2012.

Buendia, E. C., Guendehou, S., Limmeechokchai, B., Pipatti, R., Rojas, Y., Sturgiss, R., Tanabe, K., Wirth, T., Romano, D., Witi, J., Garg, A., Weitz, M. M., Cai, B., Ottinger, D. A., Dong, H., MacDonald, J. D., Ogle, S. M., Rocha, M. T., Sanchez, M. J. S., Bartram, D. M. and Towprayoon, S.: 2019 refinement to the 2006 IPCC guidelines for national greenhouse gas inventories. [online] Available from: https://www.ipcc.ch/report/2019-refinement-to-the-2006-ipcc-guidelines-for-national-greenhouse-gas-inventories/, 2019.

Bukowiecki, N., Dommen, J., Prévôt, A. S. H., Richter, R., Weingartner, E. and Baltensperger, U.: A mobile pollutant measurement laboratory - Measuring gas phase and aerosol ambient concentrations with high spatial and temporal resolution, Atmos. Environ., 36(36–37), 5569–5579, doi:10.1016/S1352-2310(02)00694-5, 2002.

Caulton, D. R., Li, Q., Bou-Zeid, E., Fitts, J. P., Golston, L. M., Pan, D., Lu, J., Lane, H. M., Buchholz, B., Guo, X., McSpiritt, J., Wendt, L. and Zondlo, M. A.: Quantifying uncertainties from mobile-laboratory-derived emissions of well pads using inverse Gaussian methods, Atmos. Chem. Phys., 18(20), 15145–15168, doi:10.5194/acp-18-15145-2018, 2018.

Chamberlain, S. D., Ingraffea, A. R. and Sparks, J. P.: Sourcing methane and carbon dioxide emissions from a small city: Influence of natural gas leakage and combustion, Environ. Pollut., 218, 102–110, doi:10.1016/J.ENVPOL.2016.08.036, 2016.

Davis, J. B. and Squires, R. M.: Detection of Microbially Produced Gaseous Hydrocarbons Other than Methane., Science, 119(3090), 381–2, doi:10.1126/science.119.3090.381, 1954.

DVGW: Technische Regel – ArbeitsblattDVGW G 260 (A), Bonn. [online] Available from: https://shop.wvgw.de/var/assets/leseprobe/508866_lp G 260.pdf, 2013.

E. K. Nam, T. E. Jensen, A. and Wallington, T. J.: Methane Emissions from Vehicles, Environ. Sci. Technol., doi:10.1021/ES034837G, 2004.

EDF: Local leaks impact global climate, [online] Available from: https://www.edf.org/climate/methanemaps (Accessed 5 November 2019), 2019.

EPA: User's guide for the industrial source guide complex (ISC3) dispersion models, volume II - Description of model algorithms., 1995.

Etheridge, D. M., Steele, L. P., Francey, R. J. and Langenfeld, R. L.: Atmospheric methane between 1000 A.D. and present: Evidence of anthropogenic emissions and climatic variability, J. Geophys. Res., 103, 979–993, doi:0148-0227/98/98JD-00923, 1998.

Etminan, M., Myhre, G., Highwood, E. J. and Shine, K. P.: Radiative forcing of carbon dioxide, methane, and nitrous oxide: A significant revision of the methane radiative forcing, Geophys. Res. Lett., 43(24), 12,614-12,623, doi:10.1002/2016GL071930@10.1002/(ISSN)1944-8007.2016GRLEDHIGH, 2016.

Federal Environment Agency: National Inventory Report for the German Greenhouse Gas Inventory 1990 – 2017. [online] Available from: https://unfccc.int/documents/194930, 2019.

von Fischer, J. C., Cooley, D., Chamberlain, S., Gaylord, A., Griebenow, C. J., Hamburg, S. P., Salo, J., Schumacher, R., Theobald, D. and Ham, J.: Rapid, Vehicle-Based Identification of Location and Magnitude of Urban Natural Gas Pipeline Leaks, Environ. Sci. Technol., 51(7), 4091–4099, doi:10.1021/acs.est.6b06095, 2017.

Fisher, R., Lowry, D., Wilkin, O., Sriskantharajah, S. and Nisbet, E. G.: High-precision, automated stable isotope analysis of atmospheric methane and carbon dioxide using continuous-flow isotope-ratio mass spectrometry, Rapid Commun. Mass Spectrom., 20(2), 200–208, 2006.

Fisher, R. E., Sriskantharajah, S., Lowry, D., Lanoisellé, M., Fowler, C. M. R., James, R. H., Hermansen, O., Lund Myhre, C., Stohl, A., Greinert, J., Nisbet-Jones, P. B. R., Mienert, J. and Nisbet, E. G.: Arctic methane sources: Isotopic evidence for atmospheric inputs, Geophys. Res. Lett., 38(21), n/a-n/a, doi:10.1029/2011GL049319, 2011.

https://doi.org/10.5194/acp-2020-657
Preprint. Discussion started: 7 August 2020

Atmospheric Chemistry and Physics Discussions

Formolo, M.: The Microbial Production of Methane and Other Volatile Hydrocarbons, in Handbook of Hydrocarbon and Lipid Microbiology, pp. 113–126, Springer Berlin Heidelberg., 2010.

Fukuda, H., Fujii, T. and Ogawa, T.: Microbial Production of C 2 -Hydrocarbons, Ethane, Ethylene and Acetylene, Agric. Biol. Chem., 48(5), 1363–1365, doi:10.1080/00021369.1984.10866323, 1984.

Gallagher, M. E., Down, A., Ackley, R. C., Zhao, K., Phillips, N. and Jackson, R. B.: Natural Gas Pipeline Replacement Programs Reduce Methane Leaks and Improve Consumer Safety, Environ. Sci. Technol. Lett., 2(10), 286–291, doi:10.1021/acs.estlett.5b00213, 2015.

Gioli, B., Toscano, P., Lugato, E., Matese, A., Miglietta, F., Zaldei, A. and Vaccari, F. P.: Methane and carbon dioxide fluxes and source partitioning in urban areas: The case study of Florence, Italy, Environ. Pollut., 164, 125–131, doi:10.1016/j.envpol.2012.01.019, 2012.

Gollakota, K. G. and Jayalakshmi, B.: Biogas (natural gas?) production by anaerobic digestion of oil cake by a mixed culture isolated from cow dung, Biochem. Biophys. Res. Commun., 110(1), 32–35, doi:10.1016/0006-291X(83)91255-X, 1983.

Heilig, G. K.: The greenhouse gas methane (CH4): Sources and sinks, the impact of population growth, possible interventions, Popul. Environ., 16(2), 109–137, doi:10.1007/BF02208779, 1994.

Helfter, C., Tremper, A. H., Halios, C. H., Kotthaus, S., Bjorkegren, A., Sue, C., Grimmond, B., Barlow, J. F. and Nemitz, E.: Spatial and temporal variability of urban fluxes of methane, carbon monoxide and carbon dioxide above London, UK, Atmos. Chem. Phys, 16, 10543–10557, doi:10.5194/acp-16-10543-2016, 2016.

Helmig, D., Rossabi, S., Hueber, J., Tans, P., Montzka, S. A., Masarie, K., Thoning, K., Plass-Duelmer, C., Claude, A., Carpenter, L. J., Lewis, A. C., Punjabi, S., Reimann, S., Vollmer, M. K., Steinbrecher, R., Hannigan, J. W., Emmons, L. K., Mahieu, E., Franco, B., Smale, D. and Pozzer, A.: Reversal of global atmospheric ethane and propane trends largely due to US oil and natural gas production, Nat. Geosci., 9(7), 490–495, doi:10.1038/ngeo2721, 2016.

Hendrick, M. F., Ackley, R., Sanaie-Movahed, B., Tang, X. and Phillips, N. G.: Fugitive methane emissions from leak-prone natural gas distribution infrastructure in urban environments, Environ. Pollut., 213, 710–716, doi:10.1016/j.envpol.2016.01.094, 2016.

Hmiel, B., Petrenko, V. V, Dyonisius, M. N., Buizert, C., Smith, A. M., Place, P. F., Harth, C., Beaudette, R., Hua, Q., Yang, B., Vimont, I., Michel, S. E., Severinghaus, J. P., Etheridge, D., Bromley, T., Schmitt, J., Faïn, X., Weiss, R. F. and Dlugokencky, E.: Preindustrial 14 CH 4 indicates greater anthropogenic fossil CH 4 emissions, Nature, 578, doi:10.1038/s41586-020-1991-8, 2020.

Hoheisel, A., Yeman, C., Dinger, F., Eckhardt, H. and Schmidt, M.: An improved method for mobile characterisation of δ^{13} CH 4 source signatures and its application in Germany, Atmos. Meas. Tech., 12(2), 1123–1139, doi:10.5194/amt-12-1123-2019, 2019.

Hopkins, F. M., Kort, E. A., Bush, S. E., Ehleringer, J. R., Lai, C.-T., Blake, D. R. and Randerson, J. T.: Spatial patterns and source attribution of urban methane in the Los Angeles Basin, J. Geophys. Res. Atmos., 121(5), 2490–2507, doi:10.1002/2015JD024429, 2016.

Hu, N., Liu, S., Gao, Y., Xu, J., Zhang, X., Zhang, Z. and Lee, X.: Large methane emissions from natural gas vehicles in Chinese cities, Atmos. Environ., 187, 374–380, doi:10.1016/j.atmosenv.2018.06.007, 2018.

IPCC: Guidelines for national greenhouse inventories. [online] Available from: https://www.ipcc-nggip.iges.or.jp/public/gl/guidelin/ch1ref8.pdf, 1996.

Jackson, R. B., Down, A., Phillips, N. G., Ackley, R. C., Cook, C. W., Plata, D. L. and Zhao, K.: Natural gas pipeline leaks across Washington, DC, Environ. Sci. Technol., 48(3), 2051–2058, doi:10.1021/es404474x, 2014.

Karion, A., Sweeney, C., Pétron, G., Frost, G., Michael Hardesty, R., Kofler, J., Miller, B. R., Newberger, T., Wolter, S., Banta, R., Brewer, A., Dlugokencky, E., Lang, P., Montzka, S. A., Schnell, R., Tans, P., Trainer, M., Zamora, R. and Conley, S.: Methane emissions estimate from airborne measurements over a western United States natural gas field, Geophys. Res. Lett., 40(16), 4393–4397, doi:10.1002/grl.50811, 2013.

Keeling, C. D.: The concentration and isotopic abundances of atmospheric carbon dioxide in rural areas, Geochim. Cosmochim. Acta, 13(4), 322–334, doi:10.1016/0016-7037(58)90033-4, 1958.

Keeling, C. D.: The concentration and isotopic abundances of carbon dioxide in rural and marine air, Geochim. Cosmochim. Acta, 24(3–4), 277–298, doi:10.1016/0016-7037(61)90023-0, 1961.

Lamb, B. K., Cambaliza, M. O. L., Davis, K. J., Edburg, S. L., Ferrara, T. W., Floerchinger, C., Heimburger, A. M. F., Herndon, S., Lauvaux, T., Lavoie, T., Lyon, D. R., Miles, N., Prasad, K. R., Richardson, S., Roscioli, J. R., Salmon, O. E., Shepson, P. B., Stirm, B. H. and Whetstone, J.: Direct and Indirect Measurements and Modeling of Methane Emissions in Indianapolis, Indiana, Environ. Sci. Technol., 50(16), 8910–8917, doi:10.1021/acs.est.6b01198, 2016.

LBEG: Geoinformation of Lower Saxony and Schleswig-Holstein, [online] Available from: https://nibis.lbeg.de/cardomap3/, 2018.

Lebel, E. D., Lu, H. S., Speizer, S. A., Finnegan, C. J. and Jackson, R. B.: Quantifying Methane Emissions from Natural Gas Water Heaters, Environ. Sci. Technol., 54(9), 5737–5745, doi:10.1021/acs.est.9b07189, 2020.

Lyon, D. R., Zavala-Araiza, D., Alvarez, R. A., Harriss, R., Palacios, V., Lan, X., Talbot, R., Lavoie, T., Shepson, P., Yacovitch, T. I., Herndon, S. C., Marchese, A. J., Zimmerle, D., Robinson, A. L. and Hamburg, S. P.: Constructing a Spatially Resolved Methane Emission Inventory for the Barnett Shale Region, Environ. Sci. Technol., 49(13), 8147–8157, doi:10.1021/es506359c, 2015.

Lyon, D. R., Alvarez, R. A., Zavala-Araiza, D., Brandt, A. R., Jackson, R. B. and Hamburg, S. P.: Aerial Surveys of Elevated Hydrocarbon Emissions from Oil and Gas Production Sites, Environ. Sci. Technol., 50(9), 4877–4886,

731 doi:10.1021/acs.est.6b00705, 2016.
732 Maazallahi, H., Fernandez, J. M., Menoud, M., Zavala-Araiza, D., Weller, Z. D., Schwietzke, S., von Fischer, J. C., Denier
733 van der Gon, H., and Röckmann, T.: MATLAB® code for evaluation of Urban Surveys, Zenodo, doi:
734 10.5281/zenodo.3928972, 2020a.
735 Maazallahi, H., Fernandez, J. M., Menoud, M., Zavala-Araiza, D., Weller, Z. D., Schwietzke, S., von Fischer, J. C., Denier
736 van der Gon, H., and Röckmann, T.: Utrecht and Hamburg city measurements data, ICOS,
737 https://doi.org/10.18160/RAJS-KZZQ, 2020b.
738 MacFarling Meure, C., Etheridge, D., Trudinger, C., Steele, P., Langenfelds, R., van Ommen, T., Smith, A. and Elkins, J.:
739 Law Dome CO2 , CH4 and N2O ice core records extended to 2000 years BP, Geophys. Res. Lett., 33(14), L14810,
740 doi:10.1029/2006GL026152, 2006.
741 McKain, K., Down, A., Raciti, S. M., Budney, J., Hutyra, L. R., Floerchinger, C., Herndon, S. C., Nehrkorn, T., Zahniser, M.
742 S., Jackson, R. B., Phillips, N. and Wofsy, S. C.: Methane emissions from natural gas infrastructure and use in the
743 urban region of Boston, Massachusetts, Proc. Natl. Acad. Sci., 112(7), 1941–1946, doi:10.1073/PNAS.1416261112,
744 2015.
745 Mitchell, A. L., Tkacik, D. S., Roscioli, J. R., Herndon, S. C., Yacovitch, T. I., Martinez, D. M., Vaughn, T. L., Williams, L.
746 L., Sullivan, M. R., Floerchinger, C., Omara, M., Subramanian, R., Zimmerle, D., Marchese, A. J. and Robinson, A.
747 L.: Measurements of Methane Emissions from Natural Gas Gathering Facilities and Processing Plants: Measurement
748 Results, Environ. Sci. Technol., 49(5), 3219–3227, doi:10.1021/es5052809, 2015.
749 Myhre, G., Shindell, D., Bréon, F. M., Collins, W., Fuglestvedt, J., Huang, J., Koch, D., Lamarque, J. F., Lee, D., Mendoza,
750 B., Nakajima, T., Robock, A., Stephens, G., Takemura, T. and Zhan, H.: Anthropogenic and Natural Radiative Forc-
751 ing. In: Climate Change 2013: The Physical Science Basis. Contribution of Working Group I to the Fifth Assessment
752 Report of the Intergovernmental Panel on Climate Change, Cambridge, United Kingdom and New York, NY, USA.
753 [online] Available from: https://www.ipcc.ch/site/assets/uploads/2018/02/WG1AR5_Chapter08_FINAL.pdf, 2013.
754 Naus, S., Röckmann, T. and Popa, M. E.: The isotopic composition of CO in vehicle exhaust, Atmos. Environ., 177, 132–142,
755 doi:10.1016/J.ATMOSENV.2018.01.015, 2018.
756 Nelson, W. A.: Statistical Methods, in Encyclopedia of Ecology, Five-Volume Set, edited by S. E. Jørgensen and B. D. Fath,
757 pp. 3350–3362, Elsevier Inc., 2008.
758 Noël, S., Weigel, K., Bramstedt, K., Rozanov, A., Weber, M., Bovensmann, H. and Burrows, J. P.: Water vapour and methane
759 coupling in the stratosphere observed using SCIAMACHY solar occultation measurements, Atmos. Chem. Phys.,
760 18(7), 4463–4476, doi:10.5194/acp-18-4463-2018, 2018.
761 O'Shea, S. J., Allen, G., Fleming, Z. L., Bauguitte, S. J.-B., Percival, C. J., Gallagher, M. W., Lee, J., Helfter, C. and Nemitz,
762 E.: Area fluxes of carbon dioxide, methane, and carbon monoxide derived from airborne measurements around
763 Greater London: A case study during summer 2012, J. Geophys. Res. Atmos., 119(8), 4940–4952,
764 doi:10.1002/2013JD021269, 2014.
765 Omara, M., Sullivan, M. R., Li, X., Subramanian, R., Robinson, A. L. and Presto, A. A.: Methane Emissions from
766 Conventional and Unconventional Natural Gas Production Sites in the Marcellus Shale Basin, Environ. Sci. Technol.,
767 50(4), 2099–2107, doi:10.1021/acs.est.5b05503, 2016.
768 Peek, C. J., Montfoort, J. A., Dröge, R., Guis, B., Baas, K., Huet, B. van, Hunnik, O. R. van and Berghe, A. C. W. M. van den:
769 Methodology report on the calculation of emissions to air from the sectors Energy, Industry and Waste, as used by
770 the Dutch Pollutant Release and Transfer Register., 2019.
771 Phillips, N. G., Ackley, R., Crosson, E. R., Down, A., Hutyra, L. R., Brondfield, M., Karr, J. D., Zhao, K. and Jackson, R. B.:
772 Mapping urban pipeline leaks: Methane leaks across Boston, Environ. Pollut., 173, 1–4,
773 doi:10.1016/j.envpol.2012.11.003, 2013.
774 Popa, M. E., Vollmer, M. K., Jordan, A., Brand, W. A., Pathirana, S. L., Rothe, M. and Röckmann, T.: Vehicle emissions of
775 greenhouse gases and related tracers from a tunnel study: CO : CO2 , N2O : CO2 , CH4 : CO2 , O2 : CO2 ratios, and
776 the stable isotopes 13C and 18O in CO2 and CO, Atmos. Chem. Phys., 14(4), 2105–2123, doi:10.5194/acp-14-2105-
777 2014, 2014.
778 Prather, M. J., Holmes, C. D. and Hsu, J.: Reactive greenhouse gas scenarios: Systematic exploration of uncertainties and the
779 role of atmospheric chemistry, Geophys. Res. Lett., 39(9), n/a-n/a, doi:10.1029/2012GL051440, 2012.
780 Rijksoverheid: Emissieregstratie. [online] Available from: http://www.emissieregistratie.nl/erpubliek/erpub/facility.aspx
781 (Accessed 9 December 2019), 2019.
782 Röckmann, T., Eyer, S., van der Veen, C., Popa, M. E., Tuzson, B., Monteil, G., Houweling, S., Harris, E., Brunner, D.,
783 Fischer, H., Zazzeri, G., Lowry, D., Nisbet, E. G., Brand, W. A., Necki, J. M., Emmenegger, L. and Mohn, J.: In situ
784 observations of the isotopic composition of methane at the Cabauw tall tower site, Atmos. Chem. Phys., 16(16),
785 10469–10487, doi:10.5194/acp-16-10469-2016, 2016.
786 Schmidt, G. A. and Shindell, D. T.: Atmospheric composition, radiative forcing, and climate change as a consequence of a
787 massive methane release from gas hydrates, Paleoceanography, 18(1), n/a-n/a, doi:10.1029/2002PA000757, 2003.
788 Schwietzke, S., Sherwood, O. A., Bruhwiler, L. M. P., Miller, J. B., Etiope, G., Dlugokencky, E. J., Michel, S. E., Arling, V.
789 A., Vaughn, B. H., White, J. W. C. and Tans, P. P.: Upward revision of global fossil fuel methane emissions based
790 on isotope database, Nature, 538(7623), 88–91, doi:10.1038/nature19797, 2016.
791 Stephenson, M. and Stickland, L. H.: Hydrogenase: The bacterial formation of methane by the reduction of one-carbon
792 compounds by molecular hydrogen, Biochem. J., 27(5), 1517–1527, doi:10.1042/bj0271517, 1933.
793 Thauer, R. K.: Biochemistry of methanogenesis: a tribute to Marjory Stephenson:1998 Marjory Stephenson Prize Lecture,

https://doi.org/10.5194/acp-2020-657
Preprint. Discussion started: 7 August 2020

Atmospheric Chemistry and Physics Discussions

Microbiology, 144(9), 2377–2406, doi:10.1099/00221287-144-9-2377, 1998.
Turner, A. J., Frankenberg, C. and Kort, E. A.: Interpreting contemporary trends in atmospheric methane, Proc. Natl. Acad. Sci., 116(8), 2805–2813, doi:10.1073/PNAS.1814297116, 2019.
Turner, D. B.: Workbook of Atmospheric Dispersion Estimates, U.S. Environmental Protection Agency. [online] Available from: https://nepis.epa.gov/Exe/ZyPDF.cgi/9101GKEZ.PDF?Dockey=9101GKEZ.PDF, 1969.
U.S. EIA: Natural gas consumptions in the United States, [online] Available from: https://www.eia.gov/energyexplained/natural-gas/use-of-natural-gas.php (Accessed 16 June 2020), 2019.
Van Ulden, A. P. and Wieringa, J.: Atmospheric boundary layer research at Cabauw, Boundary-Layer Meteorol., 78(1–2), 39–69, doi:10.1007/BF00122486, 1996.
Umezawa, T., Brenninkmeijer, C. A. M., Röckmann, T., van der Veen, C., Tyler, S. C., Fujita, R., Morimoto, S., Aoki, S., Sowers, T., Schmitt, J., Bock, M., Beck, J., Fischer, H., Michel, S. E., Vaughn, B. H., Miller, J. B., White, J. W. C., Brailsford, G., Schaefer, H., Sperlich, P., Brand, W. A., Rothe, M., Blunier, T., Lowry, D., Fisher, R. E., Nisbet, E. G., Rice, A. L., Bergamaschi, P., Veidt, C. and Levin, I.: Interlaboratory comparison of δ13C and δD measurements of atmospheric CH4 for combined use of data sets from different laboratories, Atmos. Meas. Tech., 11(2), 1207–1231, doi:10.5194/amt-11-1207-2018, 2018.
UNI MISKOLC and ETE: A register of all gas regulations and norms concerning the necessary gas quality for allowing the transport in the natural gas grid. [online] Available from: https://ec.europa.eu/energy/intelligent/projects/sites/iee-projects/files/projects/documents/redubar_a_register_of_all_gas_regulations.pdf, 2008.
US Census Bureau: U.S. and World Population Clock, [online] Available from: https://www.census.gov/popclock/ (Accessed 20 June 2020), 2020.
Weller, Z., Hamburg, S. P. and von Fischer, J. C.: A national estimate of methane leakage from pipeline mains in natural gas local distribution systems, Environ. Sci. Technol., doi:10.1021/acs.est.0c00437, 2020.
Weller, Z. D., Roscioli, J. R., Daube, W. C., Lamb, B. K., Ferrara, T. W., Brewer, P. E. and von Fischer, J. C.: Vehicle-Based Methane Surveys for Finding Natural Gas Leaks and Estimating Their Size: Validation and Uncertainty, Environ. Sci. Technol., acs.est.8b03135, doi:10.1021/acs.est.8b03135, 2018.
Weller, Z. D., Yang, D. K. and von Fischer, J. C.: An open source algorithm to detect natural gas leaks from mobile methane survey data, edited by M. Mauder, PLoS One, 14(2), e0212287, doi:10.1371/journal.pone.0212287, 2019.
West, J. J., Fiore, A. M., Horowitz, L. W. and Mauzerall, D. L.: Global health benefits of mitigating ozone pollution with methane emission controls., Proc. Natl. Acad. Sci. U. S. A., 103(11), 3988–93, doi:10.1073/pnas.0600201103, 2006.
Xu, L. and Jiang, C.: Initial desorption characterization of methane and carbon dioxide in coal and its influence on coal and gas outburst risk, Fuel, 203, 700–706, doi:10.1016/J.FUEL.2017.05.001, 2017.
Yacovitch, T. I., Herndon, S. C., Roscioli, J. R., Floerchinger, C., McGovern, R. M., Agnese, M., Pétron, G., Kofler, J., Sweeney, C., Karion, A., Conley, S. A., Kort, E. A., Nähle, L., Fischer, M., Hildebrandt, L., Koeth, J., McManus, J. B., Nelson, D. D., Zahniser, M. S. and Kolb, C. E.: Demonstration of an Ethane Spectrometer for Methane Source Identification, Environ. Sci. Technol., 48(14), 8028–8034, doi:10.1021/es501475q, 2014.
Yacovitch, T. I., Herndon, S. C., Pétron, G. P., Kofler, J., Lyon, D., Zahniser, M. S. and Kolb, C. E.: Mobile Laboratory Observations of Methane Emissions in the Barnett Shale Region, , doi:10.1021/es506352j, 2015.
Yacovitch, T. I., Neininger, B., Herndon, S. C., Van der Gon, H. D., Jonkers, S., Hulskotte, J., Roscioli, J. R. and Zavala-Araiza, D.: Methane emissions in the Netherlands: The Groningen field, Elem Sci Anth, 6(1), 57, doi:10.1525/elementa.308, 2018.
Zavala-Araiza, D., Lyon, D. R., Alvarez, R. A., Davis, K. J., Harriss, R., Herndon, S. C., Karion, A., Kort, E. A., Lamb, B. K., Lan, X., Marchese, A. J., Pacala, S. W., Robinson, A. L., Shepson, P. B., Sweeney, C., Talbot, R., Townsend-Small, A., Yacovitch, T. I., Zimmerle, D. J. and Hamburg, S. P.: Reconciling divergent estimates of oil and gas methane emissions., Proc. Natl. Acad. Sci. U. S. A., 112(51), 15597–602, doi:10.1073/pnas.1522126112, 2015.
Zazzeri, G., Lowry, D., Fisher, R. E., France, J. L., Lanoisellé, M. and Nisbet, E. G.: Plume mapping and isotopic characterisation of anthropogenic methane sources, Atmos. Environ., 110, 151–162, doi:10.1016/j.atmosenv.2015.03.029, 2015.
Zhao, W., Zhang, T., Wang, Y., Qiao, J. and Wang, Z.: Corrosion Failure Mechanism of Associated Gas Transmission Pipeline., Mater. (Basel, Switzerland), 11(10), doi:10.3390/ma11101935, 2018.
Zimmerle, D. J., Williams, L. L., Vaughn, T. L., Quinn, C., Subramanian, R., Duggan, G. P., Willson, B., Opsomer, J. D., Marchese, A. J., Martinez, D. M. and Robinson, A. L.: Methane Emissions from the Natural Gas Transmission and Storage System in the United States, Environ. Sci. Technol., 49(15), 9374–9383, doi:10.1021/acs.est.5b01669, 2015.
Zimnoch, M., Necki, J., Chmura, L., Jasek, A., Jelen, D., Galkowski, M., Kuc, T., Gorczyca, Z., Bartyzel, J. and Rozanski, K.: Quantification of carbon dioxide and methane emissions in urban areas: source apportionment based on atmospheric observations, Mitig. Adapt. Strateg. Glob. Chang., 24(6), 1051–1071, doi:10.1007/s11027-018-9821-0, 2019.

https://doi.org/10.5194/acp-2020-657
Preprint. Discussion started: 7 August 2020

Atmospheric Chemistry and Physics Discussions

856 **Table 1-Natural gas distribution network CH_4 emission categories**

Class	CH_4 Enhancement (ppm)	Equivalent Emission Rate (L/min)	Equivalent Emission Rate (≈ kg/hr)	LI Location Colour (Figure 1, Figure 2, and Figure S12)
High	>7.6	>40	>1.7	Red
Medium	1.6-7.59	6 - 40	0.3 – 1.7	Orange
Low	0.2-1.59	0.5 - 6	0.0 – 0.3	Yellow

857
858
859
860
861
862
863
864
865
866
867
868
869
870
871
872
873
874
875
876
877
878
879
880
881
882
883
884
885
886
887
888
889
890
891
892
893
894
895
896
897
898
899
900
901
902

https://doi.org/10.5194/acp-2020-657
Preprint. Discussion started: 7 August 2020

Atmospheric Chemistry and Physics Discussions

903 **Table 2- Measurements and results summaries across the study area, inside the ring in Utrecht and north Elbe in Hamburg**

Study Area				Utrecht (inside the Ring)	Hamburg (North Elbe)
≈ km street driven		Total km driven		1,000 km	1,800 km
		Driven once		220 km	900 km
		Driven more than once		780 km	900 km
≈ km street covered		Total km covered		450 km	1,200 km
		covered once		230 km	900 km
		covered more than once		220 km	300 km
LIs and emissions		Total number		81 LIs	145 LIs
		LI density		5.6 km covered/LI	8.4 km covered/LI
		Total emission rate		290 L/min	490 L/min
		Average emission rate per LI		3.6 L/min/LI	3.4 L/min/LI
		Total emission rate per year		107 t/yr	180 t/yr
LIs visited	Once	Number		16 LIs	45 LIs
		Emissions		26 L/min	68 L/min
		Average emission rate per LI		1.6 L/min/LI	1.5 L/min/LI
	More than once	Number		65 LIs	100 LIs
		Emissions		264 L/min	423 L/min
		Average emission rate per LI		4.1 L/min/LI	4.2 L/min/LI
Total LIs categorized based on von Fischer et al. (2017) categories	High (>40 L/min)	Number		1 LI	2 LIs
		Emissions		102 L/min	145 L/min
		Average emission rate per LI		101.5 (L/min/LI)	72.4 L/min/LI
		% of emissions		35 % of total emissions	30 % of total emissions
	Medium (6 – 40 L/min)	Number		6 LIs	16 LIs
		Emissions		84 L/min	176 L/min
		Average emission rate per LI		14.0 L/min/LI	11 L/min/LI
		% of emissions		30 % of total emissions	36 % of total emissions
	Low (0.5 – 6 L/min)	Number		74 LIs	127 LIs
		Emissions		105 L/min	169 L/min
		Average emission rate per LI		1.4 L/min/LI	1.3 L/min/LI
		% of emissions		36 % of total emissions	35 % of total emissions
Total LIs categorized based on OSM road classes	Level 1	Number		6 LIs	29 LIs
		Emissions		5 L/min	68 L/min
		Average emission rate per LI		0.76 L/min/LI	2.3 L/min/LI
	Level 2	Number		16 LIs	34 LIs
		Emissions		145 L/min	99 L/min
		Average emission rate per LI		9.0 L/min/LI	2.9 L/min/LI
	Level 3	Number		3 LIs	23 LIs
		Emissions		10 L/min	43 L/min
		Average emission rate per LI		3.4 L/min/LI	1.9 L/min/LI
	Residential	Number		45 LIs	52 LIs
		Emissions		93 L/min	274 L/min
		Average emission rate per LI		2.1 L/min/LI	5.3 L/min/LI
	Unclassified	Number		11 LIs	7 LIs
		Emissions		38 L/min	6 L/min
		Average emission rate per LI		3.4 L/min/LI	0.8 L/min/LI
Attribution	C2/C1 ratio analysis	Fossil (Inc. combustion)	% of emissions	93 % of total emissions	64 % of total emissions
			% of LIs	69 % of LIs	33 % of LIs
		Microbial	% of emissions	6 % of total emissions	25 % of total emissions
			% of LIs	10 % of LIs	20 % of LIs
		Unclassified	% of emissions	1 % of total emissions	11 % of total emissions
			% of LIs	21 % of LIs	47 % of LIs
	$\delta^{13}C$ and δD analysis	Fossil	% of emissions	----------	79 % of total emissions
			% of LIs	----------	38 % of LIs
		Microbial	% of emissions	----------	20 % of total emissions
			% of LIs	----------	54 % of LIs
		Other	% of emissions	----------	1 % of total emissions
			% of LIs	----------	8 % of LIs (Pyrogenic)

https://doi.org/10.5194/acp-2020-657
Preprint. Discussion started: 7 August 2020

Atmospheric Chemistry and Physics Discussions

	CH_4/CO_2 ratio analysis	Combustion	% of emissions	2 %	10 %
			% of LIs	7 %	17 %
		Other	% of emissions	98 %	90 %
			% of LIs	93 %	83 %
	C2/C1 ratio, CH_4/CO_2 ratio, and $\delta^{13}C$ - δD analyses	Fossil	% of emissions	73 %	48 %
			% of LIs	43 %	31 %
		Combustion	% of emissions	2 %	10 %
			% of LIs	7 %	17 %
		Microbial	% of emissions	8 %	35 %
			% of LIs	4 %	33 %
		Unclassified	% of emissions	16 %	7 %
			% of LIs	46 %	19%
Average emission rate per km driven				0.29 L/min/km	0.27 L/min/km
km driven / total LIs				12.5 km/LI	12.36 km/LI
Emission factors to scale-up emissions per km covered				0.64 L/min/km	0.40 L/min/km
km covered per LIs		km covered / total LIs		5.6 km/LI	8.4 km/LI
		km covered / red LIs		454.8 km/LI	611.4 km/LI
		km covered / orange LIs		75.8 km/LI	76.4 km/LI
		km covered / yellow LIs		6.1 km/LI	9.6 km/LI
km road from OSM (≈ km pipeline)				≈ 650 km	≈ 3000 km
Up-scaled methane emissions to total roads				420 L/min (≈150 t/yr)	1,200 L/min (≈440 t/yr)
Bootstrap emission rate estimate and error				420 ± 120 L/min	1,200 ± 170 L/min
Population in study area				≈ 0.28 million	≈ 1.45 million
Average LIs emissions per capita (kg/yr/capita)				0.54 ± 0.15	0.31 ± 0.04
Yearly natural gas consumption				≈ 0.16 bcm/yr	≈ 0.75 bcm/yr
Fossil emission factors	C2/C1 ratio attribution analysis		Average emission rate per km gas pipeline	0.60 ± 0.2 L/min/km	0.26 ± 0.04 L/min/km
			Average emission rates per capita	0.50 ± 0.14 kg/yr/capita	0.20 ± 0.03 kg/yr/capita
	$\delta^{13}C$ and δD attribution analysis		Average emission rates per km gas pipeline	----------	0.32 ± 0.05 L/min/km
			Average emission rates per capita	----------	0.25 ± 0.04 kg/yr/capita
	C2/C1 ratio, CH_4/CO_2 ratio, and $\delta^{13}C$ - δD analyses		Average emission rates per km gas pipeline	0.47 ± 0.14 L/min/km	0.19 ± 0.03 L/min/km
			Average emission rates per capita	0.39 ± 0.11 kg/yr/capita	0.15 ± 0.02 kg/yr/capita
			Average emission rates / yearly consumption	0.10 – 0.12 %	0.04 – 0.07 %

https://doi.org/10.5194/acp-2020-657
Preprint. Discussion started: 7 August 2020

Atmospheric Chemistry and Physics Discussions

Table 3- CH_4 Emissions from larger facilities in Utrecht and Hamburg estimated with the Gaussian Plume model

Facility	Emission rate (t/yr)
Utrecht	
Waste Water Treatment Plant (52.109791 °N, 5.107605 °E)	160 ± 80 (n = 5)
Hamburg	
F: Compost and Soil Company (53.680233 °N, 10.053751 °E)	60 ± 40 (n = 5)
Upstream D1: 53.468774 °N,10.184481 °E (separator) D2: 53.468443 °N,10.187408 °E (storage tanks) D3: 53.466694 °N,10.180647 °E (oil well)	 D1: 4.4 ± 3.6 (n = 5) D2: 5.2 ± 2.9 (n = 5) D3: 4.8 ± 3.9 (n = 5)

https://doi.org/10.5194/acp-2020-657
Preprint. Discussion started: 7 August 2020

Atmospheric Chemistry and Physics Discussions

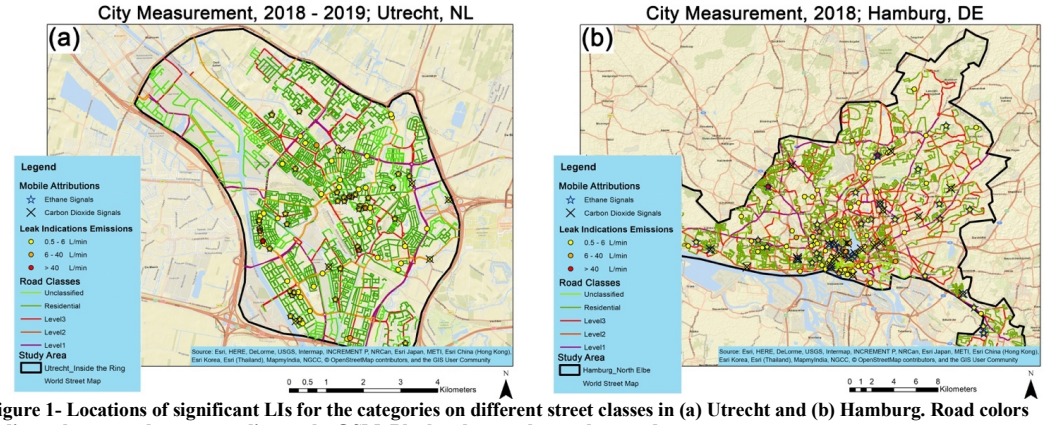

Figure 1- Locations of significant LIs for the categories on different street classes in (a) Utrecht and (b) Hamburg. Road colors indicate the street classes according to the OSM. Black polygons show urban study areas.

https://doi.org/10.5194/acp-2020-657
Preprint. Discussion started: 7 August 2020

Atmospheric Chemistry and Physics Discussions

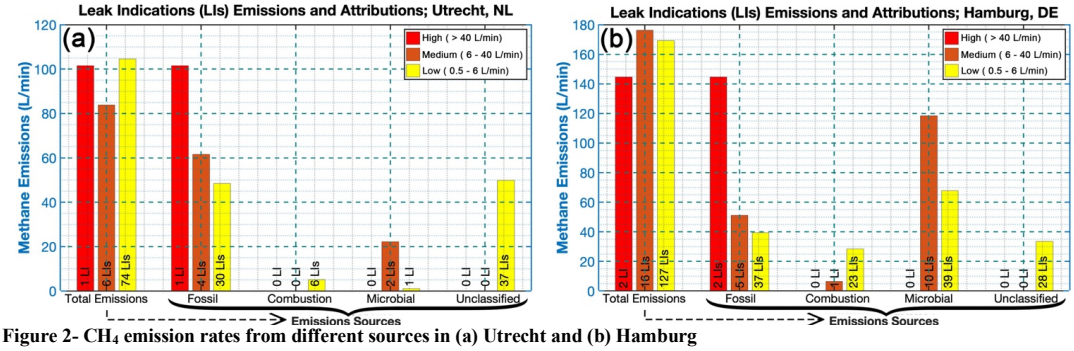

Figure 2- CH_4 emission rates from different sources in (a) Utrecht and (b) Hamburg

https://doi.org/10.5194/acp-2020-657
Preprint. Discussion started: 7 August 2020

Atmospheric Chemistry and Physics Discussions

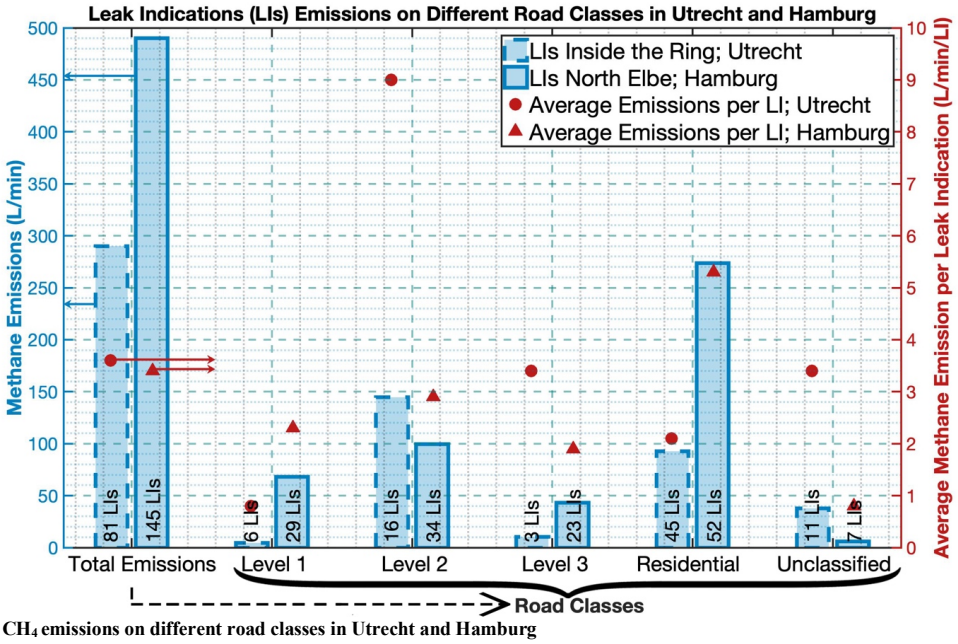

Figure 3- CH_4 emissions on different road classes in Utrecht and Hamburg

https://doi.org/10.5194/acp-2020-657
Preprint. Discussion started: 7 August 2020

Atmospheric Chemistry and Physics Discussions

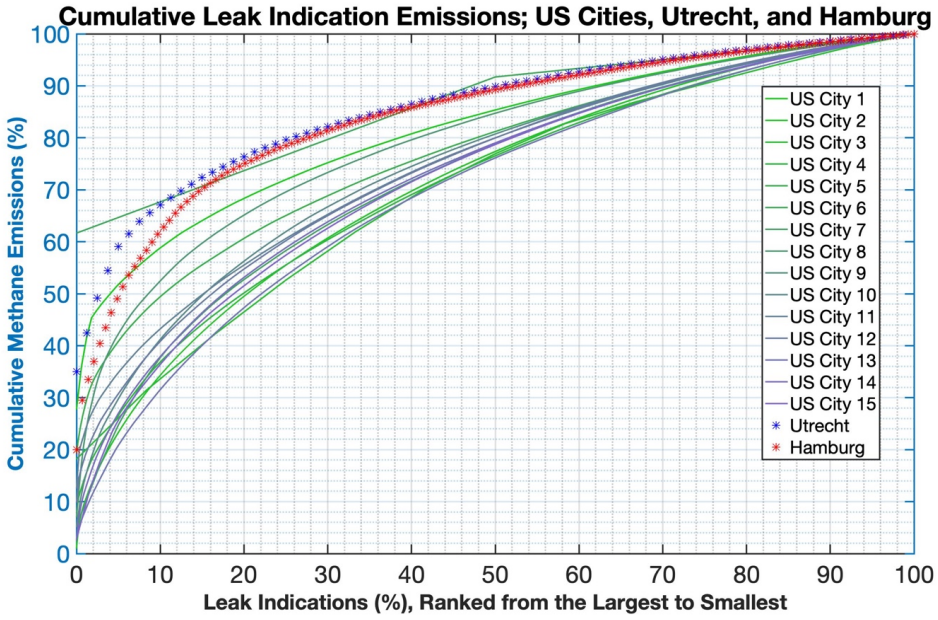

Figure 4- Cumulative plot of CH_4 emissions across US cities, Utrecht, and Hamburg; datasets for the US cities are from Weller et al. (2019)

https://doi.org/10.5194/acp-2020-657
Preprint. Discussion started: 7 August 2020

Atmospheric Chemistry and Physics Discussions

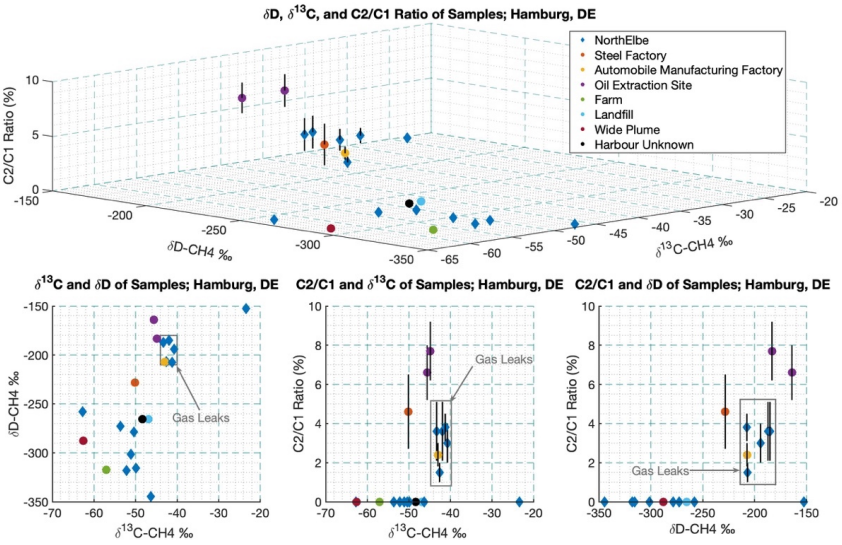

Figure 5- Results from the attribution measurements in Hamburg: C2/C1 ratios, and isotopic signatures ($\delta^{13}C$ and δD) of air samples collected

https://doi.org/10.5194/acp-2020-657
Preprint. Discussion started: 7 August 2020

Atmospheric Chemistry and Physics Discussions

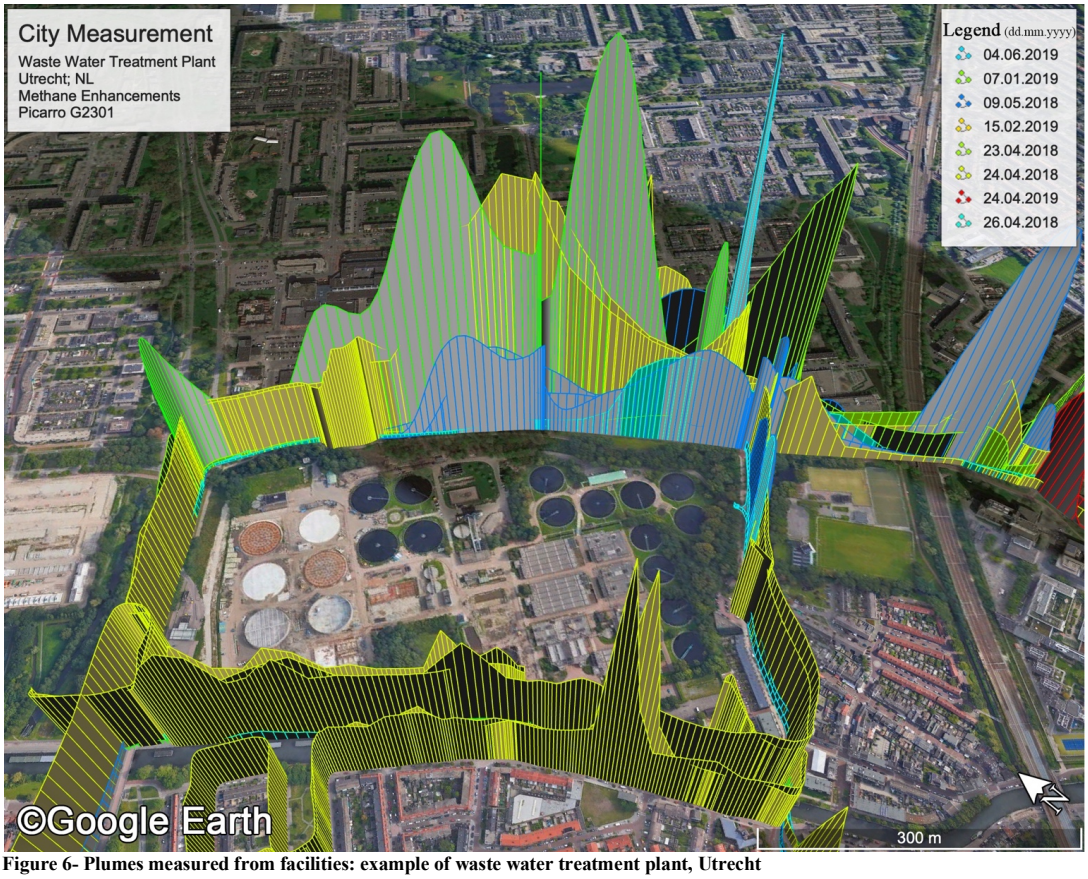

Figure 6- Plumes measured from facilities: example of waste water treatment plant, Utrecht

https://doi.org/10.5194/acp-2020-657
Preprint. Discussion started: 7 August 2020

Atmospheric Chemistry and Physics Discussions

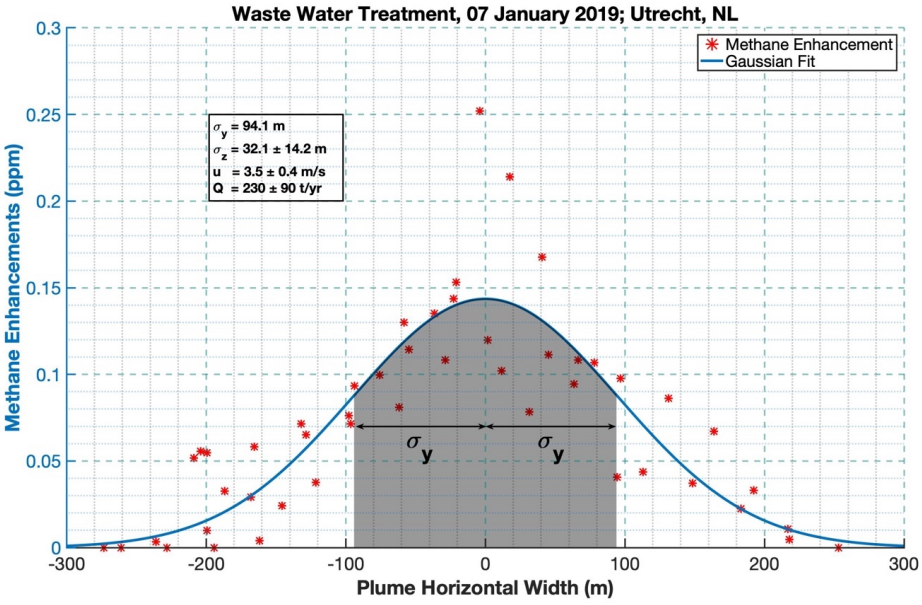

Figure 7- Gaussian curve fitted to some transects downwind the waste water treatment plant in Utrecht